THE UNIVERSITY OF MICHIGAN

INDUSTRY PROGRAM OF THE COLLEGE OF ENGINEERING

BEHAVIOR AND MAXIMUM STRENGTH OF METAL COLUMNS

Richard H. Batterman
Bruce G. Johnston

May, 1966

IP-740

TABLE OF CONTENTS

LIST OF FIGURES

LIST OF FIGURES (CONT'D)

LIST OF FIGURES (CONT'D)

SYNOPSIS

By means of digital computer simulation the complete load-deformation history of a column may be obtained. Thus about one thousand simulated column tests have provided a basis to establish systematically the maximum strength and study the behavior of both straight and initially crooked columns for various yield point steels and a typical aluminum alloy. The effects of residual stress, alone or in combination with initial crookedness, are systematically evaluated for steel columns.

INTRODUCTION

If an initially straight prismatic column with either homogeneous or symmetric stress-strain characteristics is loaded axially, the column will remain straight until it reaches the critical load at which it can be in equilibrium in either a straight or slightly bent configuration. Since any real column has some initial imperfection, the buckling of a perfect column may be thought of as a limiting behavior that is approached as the imperfections are reduced toward zero. At the critical load the column will begin to deflect laterally* at either a constant load or with a load gradient depending upon whether behavior is elastic or inelastic.

If all of the material is linearly elastic up to the critical load, the average critical stress is given by the Euler equation:

$$\sigma_E = \frac{\pi^2 E}{\left(\frac{KL}{r}\right)^2} \tag{1}$$

where E = Young's Modulus of Elasticity.

L = Length of column.

K = The equivalent length factor, such as to make KL equal to the half wave length of the column deflection curve.

r = Radius of gyration of the cross section.

---

* It is assumed that the cross section is such as will preclude torsional buckling.

If the material has not been linearly elastic up to the buckling load, the critical stress is

$$\sigma_C = \frac{\pi^2 E f(\eta)}{\left(\frac{KL}{r}\right)^2} \tag{2}$$

where $\eta = \frac{E_T}{E}$

E_T is the slope of the stress-strain curve at the instant of buckling. If the inelastic behavior has been homogeneous, i.e., identical at all points within the column,

$$f(\eta) = \eta \tag{3}$$

and Equation (2) in this case is commonly termed the "tangent-modulus" stress. Lack of homogeneity of inelastic behavior may be due to non-uniformity of stress-strain characteristics or to the presence of initial residual stresses, or both.

A full discussion of the development of the foregoing equations with examples of various functions $f(\eta)$ will be found in Reference (1).

As detailed in Reference (1), the effects of nonlinear stress-strain properties, residual stress, and initial crookedness have been studied extensively heretofore as separate parameters. The primary purpose of the present investigation, as made possible by means of the digital computer, has been the study of these effects in combination, not only in the elastic range but up to and beyond the maximum load in the inelastic range of behavior.

---

(1) Column Research Council Guide to Design Criteria for Metal Compression Members, 2nd Ed., John Wiley and Sons, 1966.

For aluminum alloy columns, inelastic behavior has been assumed to be homogeneous, with stress-strain relations simulated as typical of Aluminum Alloy 6061-T6 having a yield stress of 40 ksi. For steel columns, simple elasto-plastic stress-strain relations have been assumed, with yield stress levels of 36, 60, and 100 ksi in combination with maximum compressive residual stresses of 10 and 20 ksi.

Initial crookedness is introduced in this study by assuming the initial shape to be a half-sine wave with amplitude of 0.0005, 0.001, 0.002 and 0.004 times the length. The amplitude of 0.001L is representative of allowable tolerances for camber or sweep of rolled steel or extruded aluminum sections used as columns.

Column analysis, adapted to the numerical incremental treatment by means of a digital computer, will be covered briefly. The results of simulated tests of aluminum alloy columns are then discussed. Finally the results of simulated tests of steel columns are presented, involving three yield points, and varying amounts of residual stress with or without various levels of initial crookedness. In addition, special studies include the effect of residual stress pattern and the effect of assuming that the shape of the column axis remains that of a half-sine wave throughout the inelastic range of behavior.

MATHEMATICAL MODEL

A conceptual representation of the column considered in this study is shown in Figure 1. Due to initial crookedness, the centroidal axis of the column is displaced a distance $v_o(z)$ from the line of action of the loads. As load is applied, additional displacement $v(z)$ takes place due to the bending strains induced by virtue of the initial displacement. At any stage of loading, the load, moment, and deflection are related by equilibrium, as follows:

$$M(z) = P \cdot [v_o(z) + v(z)] \tag{4}$$

Referring to Figure 2*, a typical unit length segment of the column is subjected to a strain distribution due to bending. The strain is assumed to vary linearly across the section, proportional to the distance from the neutral axis, $y - c$. The strain is, therefore,

$$\epsilon = \frac{d^2v}{dz^2} \cdot (y - c) \tag{5}$$

For the general stress-strain relation, $\sigma(\epsilon)$, the load, P, and the resisting moment, M, may be expressed as follows:

$$P = \int_o^d \sigma(\epsilon) \cdot b \cdot dy \text{ (constant throughout the length)} \tag{6}$$

$$M = \int_o^d \sigma(\epsilon) \cdot (y - y_o) \cdot b \cdot dy \tag{7}$$

Substituting Equation (5) into Equations (6) and (7), and the latter into Equation (4), the following equation results:

---

* As drawn, for graphical clarity, the strains shown are the mirror image of the actual compressive strains to be expected in the column.

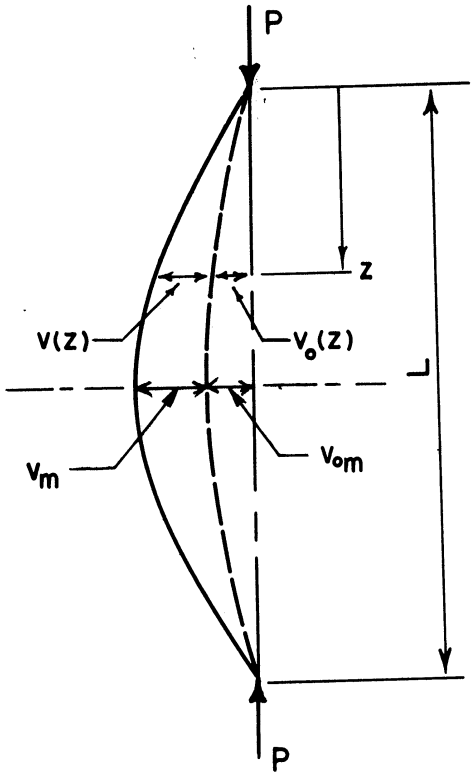

Figure 1. Initially Crooked Column

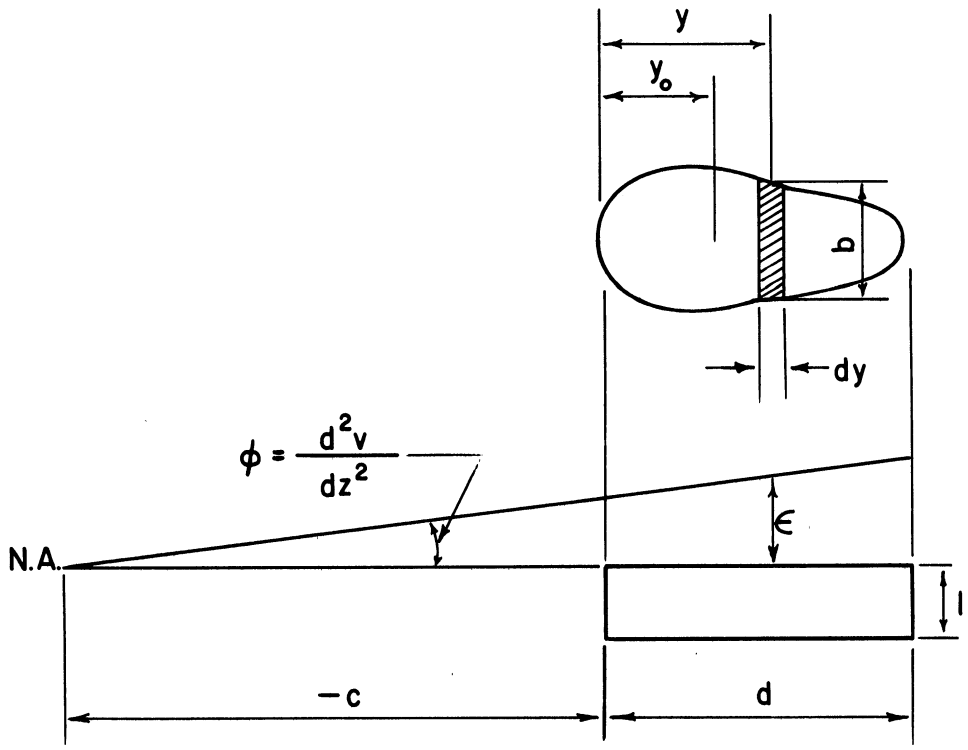

Figure 2. Strain Distribution in Typical Section

$$\int_0^d \sigma\left(\frac{d^2v}{dz^2} \cdot (y - c)\right) \cdot (y - y_o) \cdot b \cdot dy =$$

$$[v_o + v] \int_0^d \sigma\left(\frac{d^2v}{dz^2} \cdot (y - c)\right) \cdot b \cdot dy \qquad (8)$$

In general, Equation (8) is solved by finding the unknown functions $v(z)$ and $c(z)$. In the linearly elastic case, $\sigma(\epsilon) = E \cdot \epsilon$, Equation (8) reduces to

$$EI \frac{d^2v}{dz^2} = P \cdot (v_o + v) \qquad (9)$$

where E = Young's Modulus.

I = Moment of Inertia.

For certain initial crookedness functions, $v_o(z)$, and section variations, $I(z)$, closed solutions of Equation (9) can be found. Numerical methods can be used for more difficult cases.

In the inelastic case, the stress is a complex function of the strain history and the initial residual stress, σ_r, at the point in question. This is true not only because of the non-linear aspect of the stress-strain relationship, but also because of the irreversible nature of this relationship with respect to strain regression. Because of the resulting mathematical difficulties, plus the desire to be able to study a variety of functions $v_o(z)$, $d(z)$, $b(z,y)$ $\sigma_r(y)$, and $\sigma(\epsilon)$, a numerical-incremental analysis was chosen. This procedure involves calculating and recording the complete stress-strain distribution at a number of discrete stations along the column length during small finite increments of load and lateral deflection. To avoid convergence difficulties in the vicinity of the maximum load, the increment in midpoint deflection, rather than the load, is taken as the independent variable. Numerical integration is used to evaluate the load, moments, and deflection curves during each increment.

The values of v and c are considered at $m-1$ equidistantly spaced $(\Delta z = L/m)$ stations along the column length, and are represented by

$$v(z) \simeq v(z_i) \equiv v_i$$

and (10)

$$c(z) \simeq c(z_i) \equiv c_i$$

The unknown values of v and c can be found for each increment by a trial-and-error solution of Equation (8) as explained in the next section.

Associated with v is the "angle change" function

$$\frac{d^2v(z)}{dz^2} \simeq \phi\ (z_i) = \phi_i$$

The vectors, $\bar{\phi}$ and $\bar{v}$, can be related linearly as follows:

$$v_i = \sum_{j-1}^{m-1} R_{i,j} \cdot \phi_j \qquad (11)$$

The matrix, $\bar{R}$, can be derived as the product of two matrices, $\bar{A}$ and $\bar{B}$, which are defined below (See Figure 3). $\bar{\theta} = \bar{A}\,\bar{\phi}$ (the elements of $\bar{\theta}$ are concentrated angle changes)

$$\bar{v} = \bar{B}\,\bar{\theta} = \bar{B}\,\bar{A}\,\bar{\phi} = \bar{R}\,\bar{\phi}$$

Thus $\bar{R} = \bar{B}\,\bar{A}$.

For a column of length L and $m = 4$, for example, $\bar{A}$ and $\bar{B}$ can be defined as follows. Using Newmark's method,

$$\bar{A} = \begin{bmatrix} 10 & 1 & 0 \\ 1 & 10 & 1 \\ 0 & 1 & 10 \end{bmatrix} \frac{L}{48} \qquad (12)$$

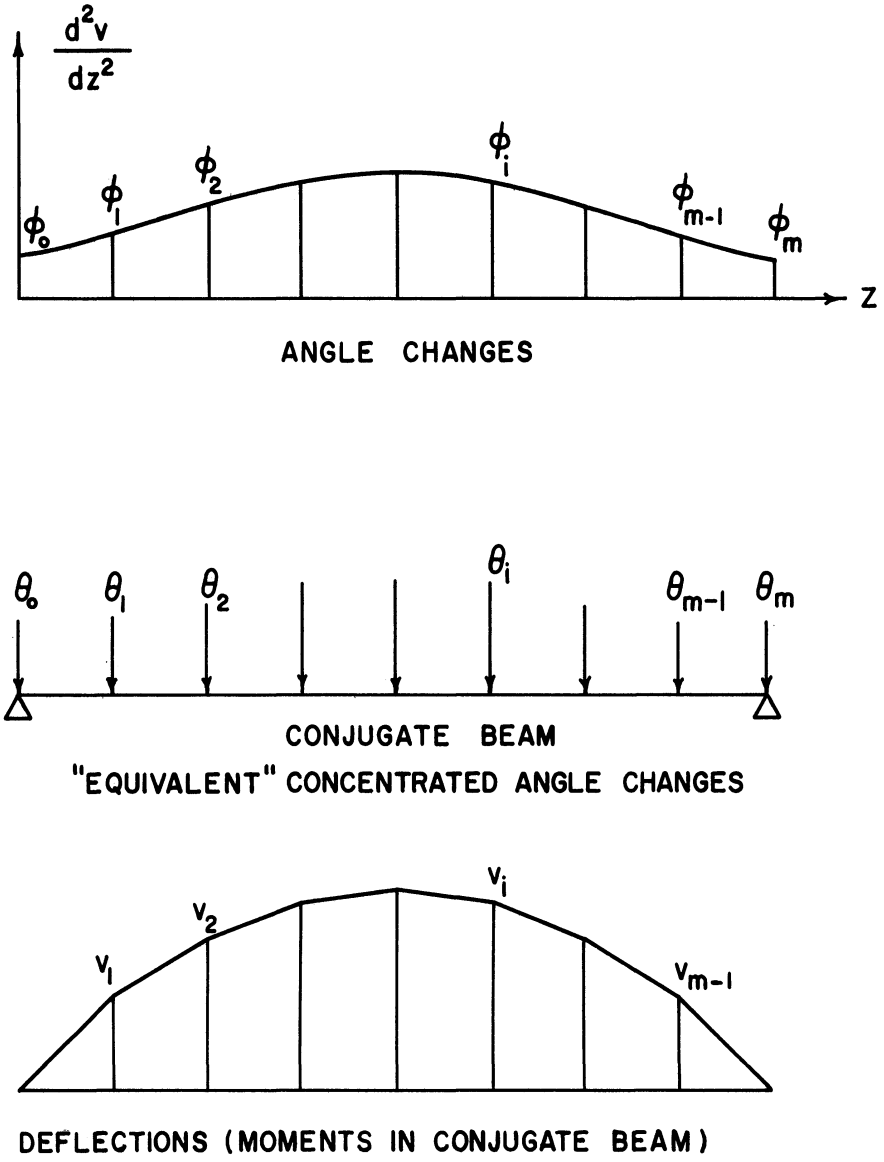

Figure 3. Numerical Relationship between Angle Changes and Deflections

and by the conjugate beam method,

$$\overline{B} = \begin{bmatrix} 3 & 2 & 1 \\ 2 & 4 & 2 \\ 1 & 2 & 3 \end{bmatrix} \frac{L}{16} \qquad (13)$$

Thus,

$$R = \begin{bmatrix} 32 & 24 & 12 \\ 24 & 44 & 24 \\ 12 & 24 & 32 \end{bmatrix} \frac{L^2}{768} = \begin{bmatrix} 8 & 6 & 3 \\ 6 & 11 & 6 \\ 3 & 6 & 8 \end{bmatrix} \frac{L^2}{192} \qquad (14)$$

COMPUTATIONAL PROCEDURE

The procedure begins by establishing the load at which bending begins. For straight columns ($v_o = 0$) bending begins at the tangent modulus load, found parametrically in terms of the strain in the equation

$$\int_o^d \sigma(\epsilon) \cdot b \cdot dy - \frac{\pi^2}{L^2} \cdot \int_o^d E_t(\epsilon) \cdot (y - \frac{d}{2})^2 \cdot b \cdot dy = 0$$

For $v_o \neq 0$, bending begins immediately at $P = 0$.

For each increment of deflection, the initial shape of the incremental deflection curve must be assumed and corrected as necessary. For example, a good initial guess would be the half-wave of a sine curve. At each station along the column it is possible to solve Equation (8) for c if v is known or assumed. When the correct deflected shape has been assumed, the values of ΔP calculated at each of the sections will be equal. Normally, for the first trial deflection curve, the ΔP values will be unequal and the curve must be corrected. If the ΔP value at a station is below the average of all ΔP's, a greater angle change should be assumed for that station, whereas, if it is above the average, a smaller angle change should be assumed. It was found that the following equation gave a good revised estimate of the angle change value.

$$\phi_i \rightarrow \phi_i \frac{\Delta P_{avg} + Q}{\Delta P_i + Q} \tag{15}$$

The term Q was used to optimize the rate of convergence.

When the deflection curve has been established such that the deviations of the ΔP values from the mean are below a desired value, Equation (8) is considered to be solved for that particular deflection increment. For the next increment, the incremental deflection curve from the preceding increment is assumed and corrected as necessary.

Further increments are thus considered until as much as desired of the load-deflection curve has been established. A flow diagram of the procedure is given in Figure 4.

COMPUTER PROGRAM

The incremental procedure has been programmed for an IBM 7090 computer. Idealized stress-strain relations shown qualitatively in Figure 5 were assumed. For steel, the stress increment diagrams consisted of triangular and trapezoidal shapes which allowed a direct, rather than approximate, integration for load and moment. The stress-strain relations for aluminum alloys were approximated by algebraic expressions, and the integration of stress diagrams for load and moment was accomplished numerically by Simpson's "one-third" method. Residual stresses were not considered in aluminum alloy columns because of the straightening operation performed on extruded sections involving a longitudinal stretch of about one per cent. In the steel wide flange sections, residual stress patterns that varied linearly or parabolically (Figure 6) were considered. In both metals, the wide flange section was assumed to be of constant section throughout the column length.

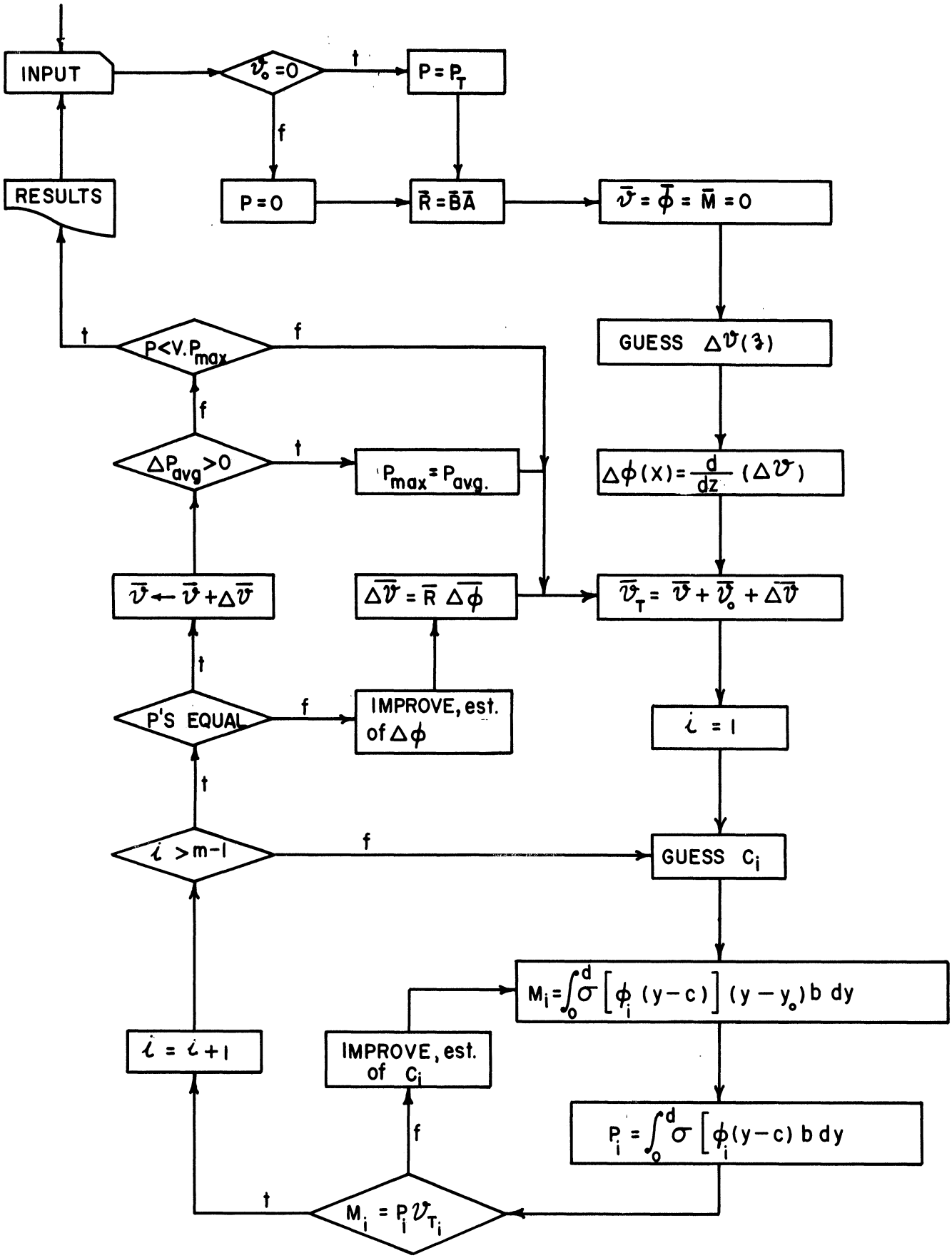

Figure 4. Flow Diagram for Incremental Column Analysis

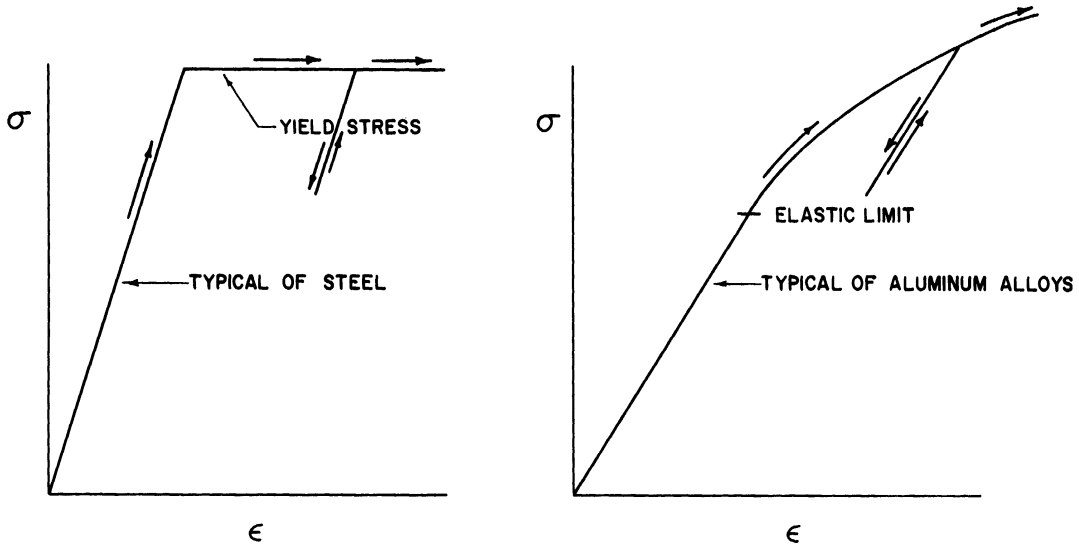

Figure 5. Types of Stress-Strain Relations

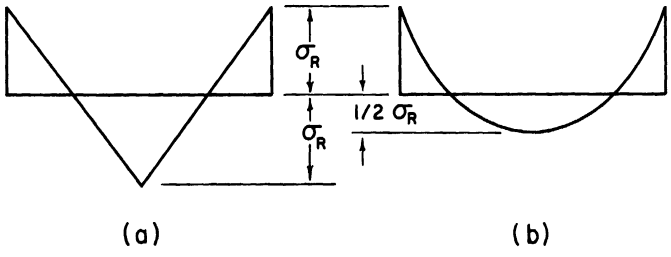

Figure 6. Residual Stress Patterns Assumed in Flanges of Wide Flange Steel Sections

BEHAVIOR OF ALUMINUM ALLOY COLUMNS

Typical stress-strain properties of Alloy 6061-T6 were used for the simulated aluminum alloy column tests. The stress-strain curve, representing the average of a large number of mechanical tests, and the arithmetic expressions used to approximate this curve are plotted in Figure 7. By considering strong and weak-axis bending of a wide flange shape (Figure 8) the practical range of shape effect is approximately covered. A total of 110 combinations of parameters were studied systematically, involving axes of bending, L/r, and v_o/L, as follows:

Axis of Bending	L/r	v_o/L
x - x	20	0
y - y	30	.0005
	40	.0010
	50	.0020
	60	.0040
	70	
	80	
	90	
	100	
	120	
	160	

In studying the buckling behavior of columns with various degrees of initial crookedness it is of interest to examine the stress distributions at a number of sections along the column length at various load levels. Inelastic buckling of an initially straight column is accompanied by an increase in column load. Thus there must be strain reversal at the mid-point of the column at the onset of buckling to provide an equilibriating increment of internal resisting moment. Reference (1) describes the development of column buckling theory from the work of Euler in 1759 down to the present

time, with emphasis on the recent developments made possible by concepts introduced by Shanley[2] in 1947. For initially crooked columns which begin to bend at $P = 0$, strain reversal will not necessarily occur as bending begins. These facts are illustrated in Figure 9 which shows successive stress distributions for a straight and a crooked column of the same length. Note that for the straight column, strain reversal does occur immediately in the central region of the column, but not at sections near the ends.

As bending progresses, the relative neutral strain axes move across the section in a direction away from the convex toward the concave side of the column. This movement is most rapid at sections away from the midpoint. In fact, as shown in Figure 10, the extent of strain regression is apt to be greater for these sections than for the midpoint at an advanced state of bending. This leads to an interesting fact concerning the shape of the deflection curve. Because of the influence of the elastic modulus, sections that initially undergo strain regression have a greater bending stiffness than those that do not. This naturally affects the shape of the deflection curve which would be a half sine-wave if the bending stiffness were uniform along the column length. Figure 11 shows that, for initially straight columns, the shape is somewhere between a half sine-wave and a parabola for the first small finite deflection. As bending progresses the shape becomes more sinusoidal $(v(L/4)/v(L/2) = \sqrt{2}/2)$ and finally becomes more sharply bent at the center than a half sine-wave.

---

(2) Shanley, F. R., "Inelastic Column Theory", J. Aero Sci., Vol. 14, No. 5, May, 1947, p. 261

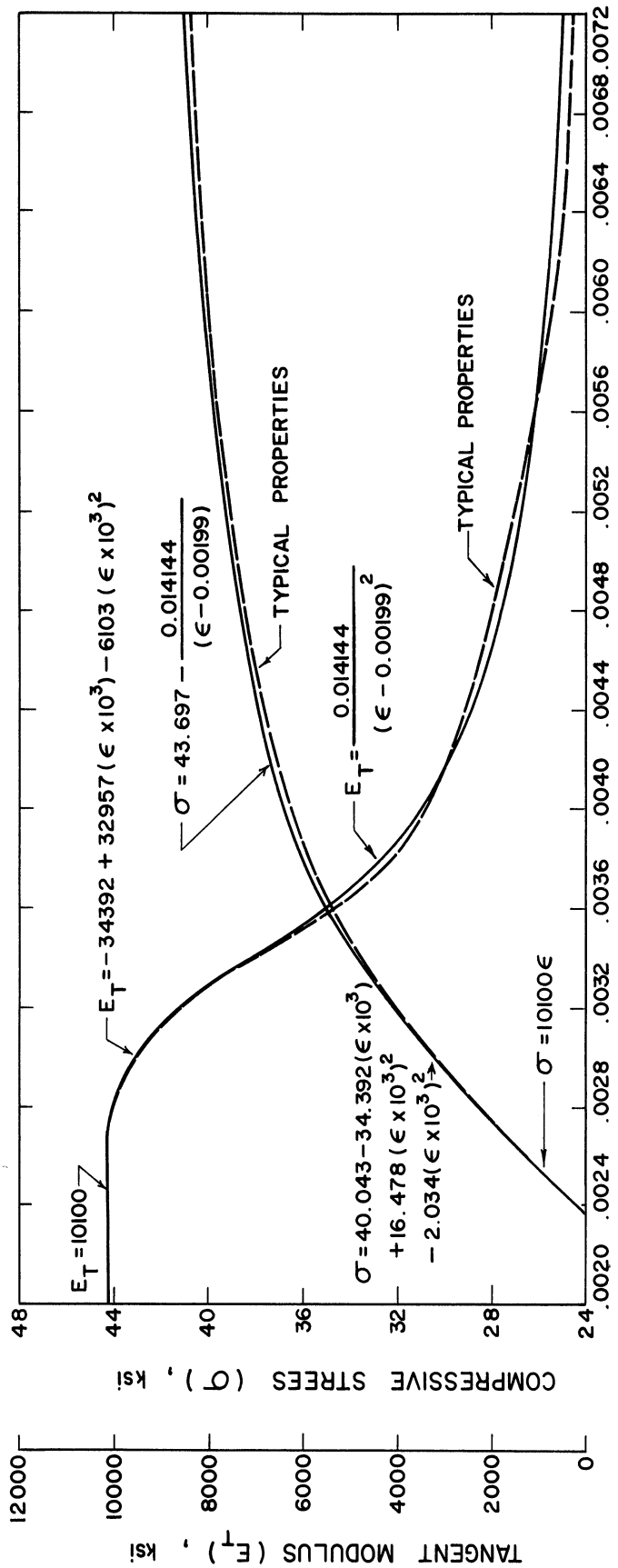

Figure 7. Stress-Strain and Tangent Modulus-Strain Relationships Typical of Aluminum Alloy 6061-T6

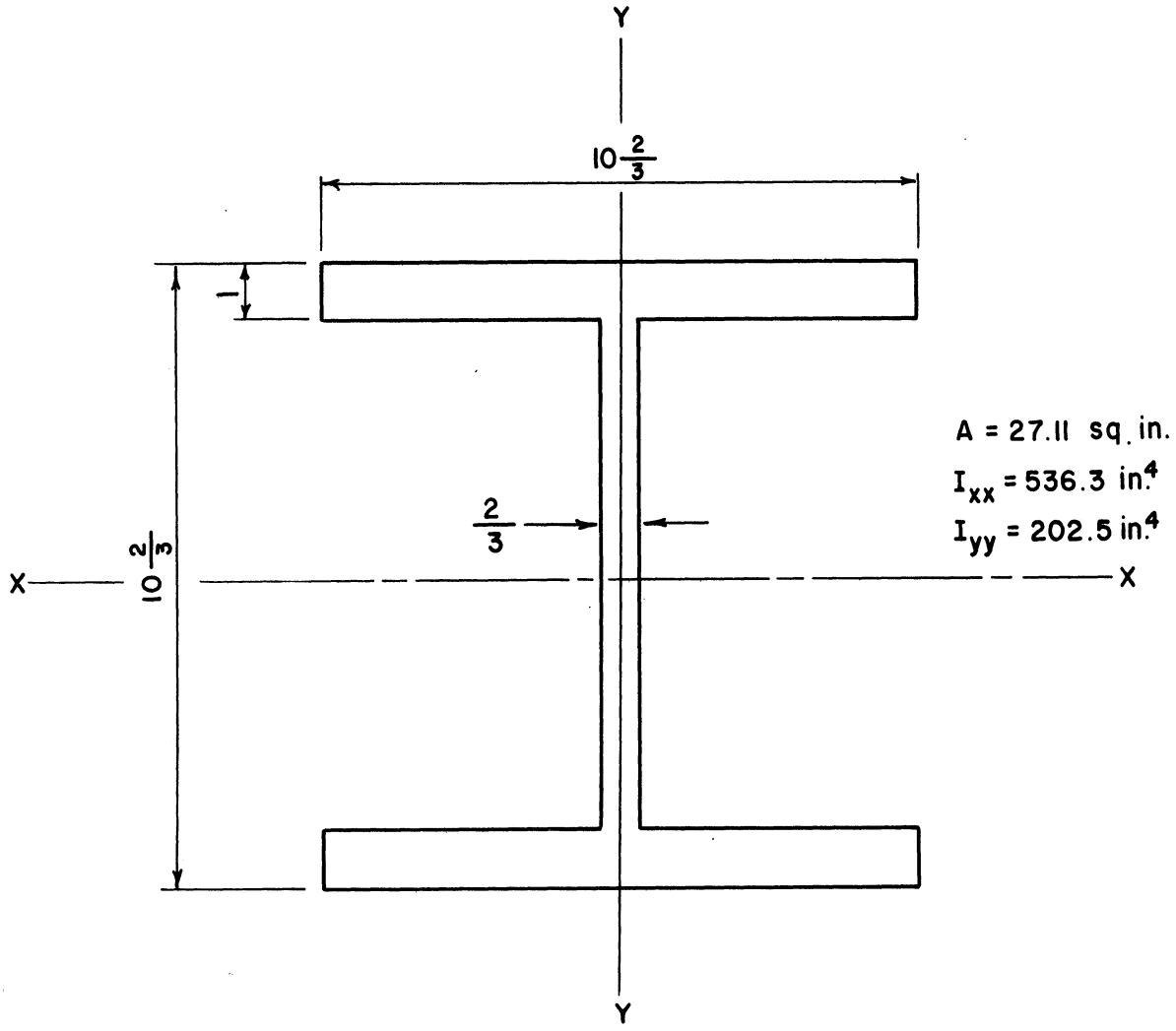

Figure 8. Proportions of Wide Flange Shapes Assumed for Aluminum Alloy Columns

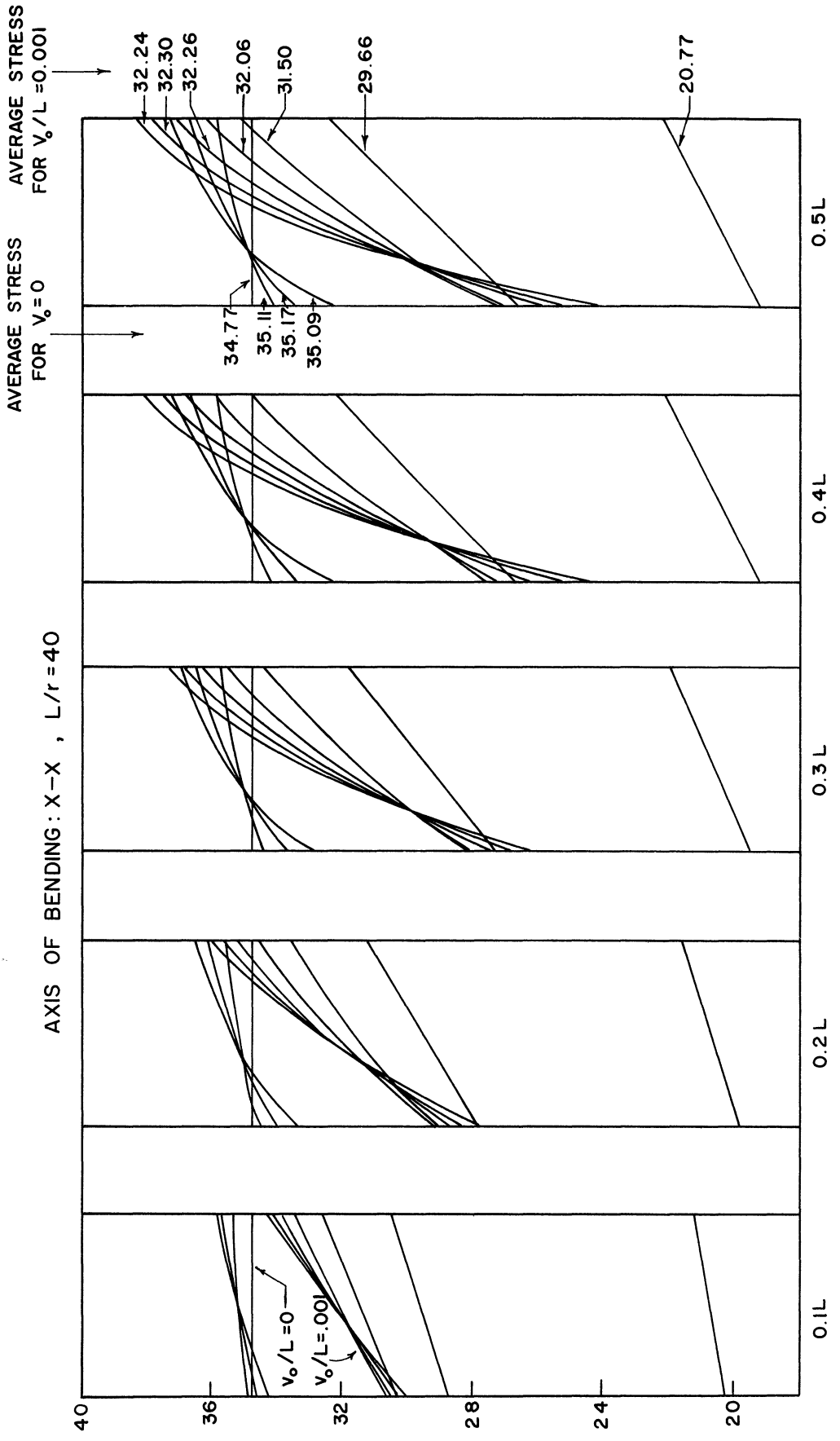

Figure 9. Stress Distributions at Various Loads Compared for Initially Straight and Initially Crooked Aluminum Alloy Columns

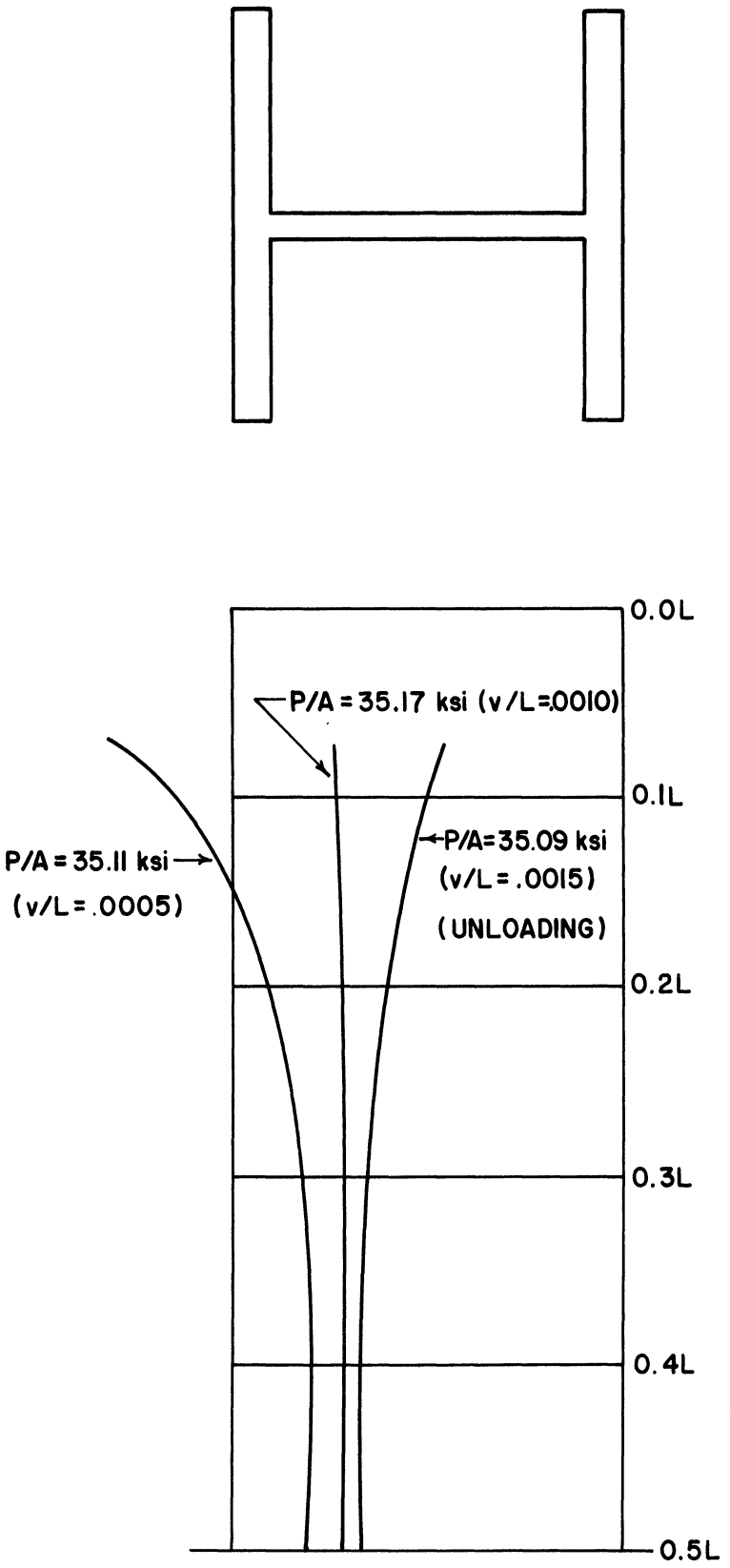

Figure 10. Initial Strain Regression Regions Near Maximum Load for an Initially Straight Aluminum Alloy Column

For crooked columns whose initial imperfection is in the shape of a half-sine wave, the deflection curve remains sinusoidal until the proportional limit is exceeded at some point. It then begins to bend more and more rapidly at sections near the center because of the decreasing bending stiffness at these sections.

Plots of load versus mid-point deflection provide an excellent means for visualizing column behavior. A number of these plots for various combinations of slenderness ratio and crookedness are given in Figures 12, 14, 15, and 16. Of special interest is Figure 12 which plots average stress versus mid-point deflection divided by length for three initially straight columns with L/r of 20, each having a different distribution of cross sectional shape about the axis of bending. All three begin to bend at the same average tangent modulus stress. As bending progresses, each gains additional load, the wide flange bent about the weak axis gaining the most, the same shape bent about the strong axis gaining the least, and the rectangular shape performing somewhere between these extremes. To show this increase in strength for other slenderness ratios, the ratio of ultimate load to tangent modulus load is plotted against L/r in Figure 13 for weak and strong axis bending of the wide flange shape. The figure shows that the weak axis maintains this superior reserve over the entire inelastic region (L/r from 0 to 60). More importantly, however, the reserve strength is very small compared to the tangent modulus load - a maximum of about two per cent for weak axis bending. This fact further justifies use of the tangent modulus load as a basis for estimating the strength of initially straight columns.

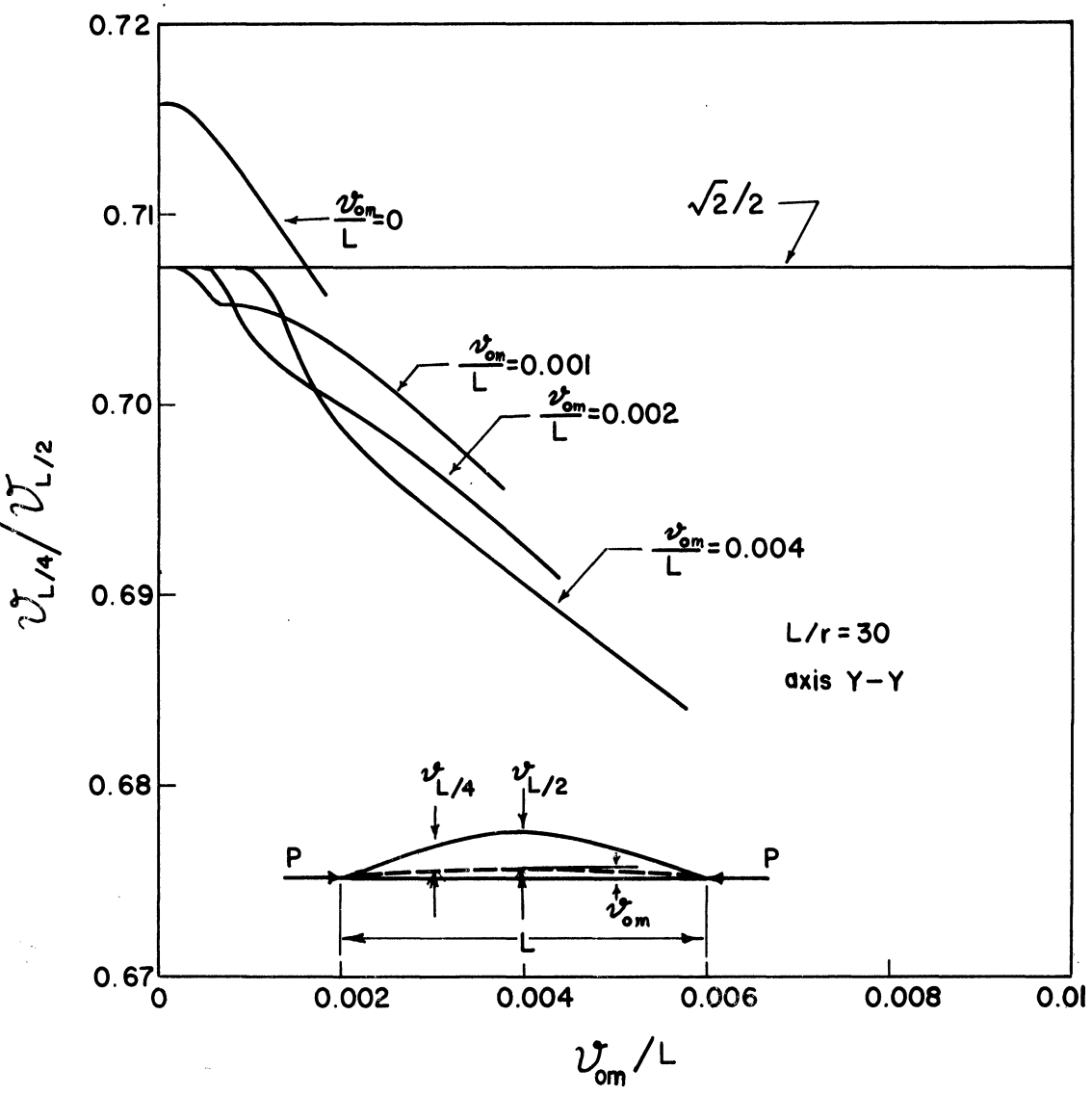

Figure 11. Ratio of Quarter-Point to Mid-point Deflection

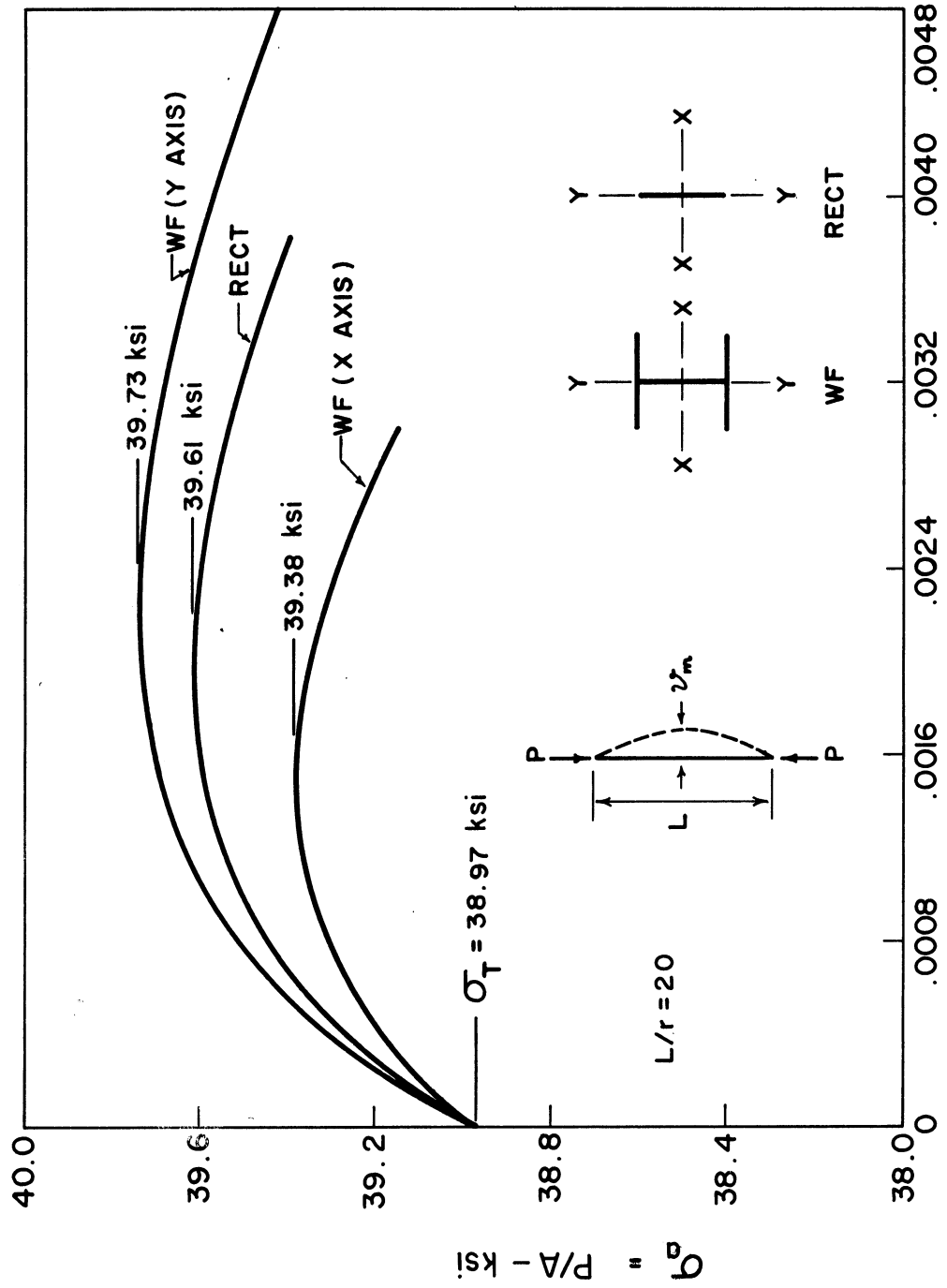

Figure 12. Load-Deflection of Initially Straight Columns with Different Cross Section

The effect of crookedness on column strength can be seen in Figures 14, 15, and 16. These are for strong axis bending (about x - x) of WF shapes. Very similar families of curves could also be shown for weak axis bending. The strength is increasingly reduced with increasing initial imperfection, and there is a marked effect on the magnitude of deflection required before ultimate strength is reached.

A summary of strengths obtained with the mathematical model is provided by the column curves plotted in Figure 17. The reduction in strength due to crookedness plotted in Figure 18 shows that the greatest effect is on columns which, when straight, buckle at stresses near the proportional limit.

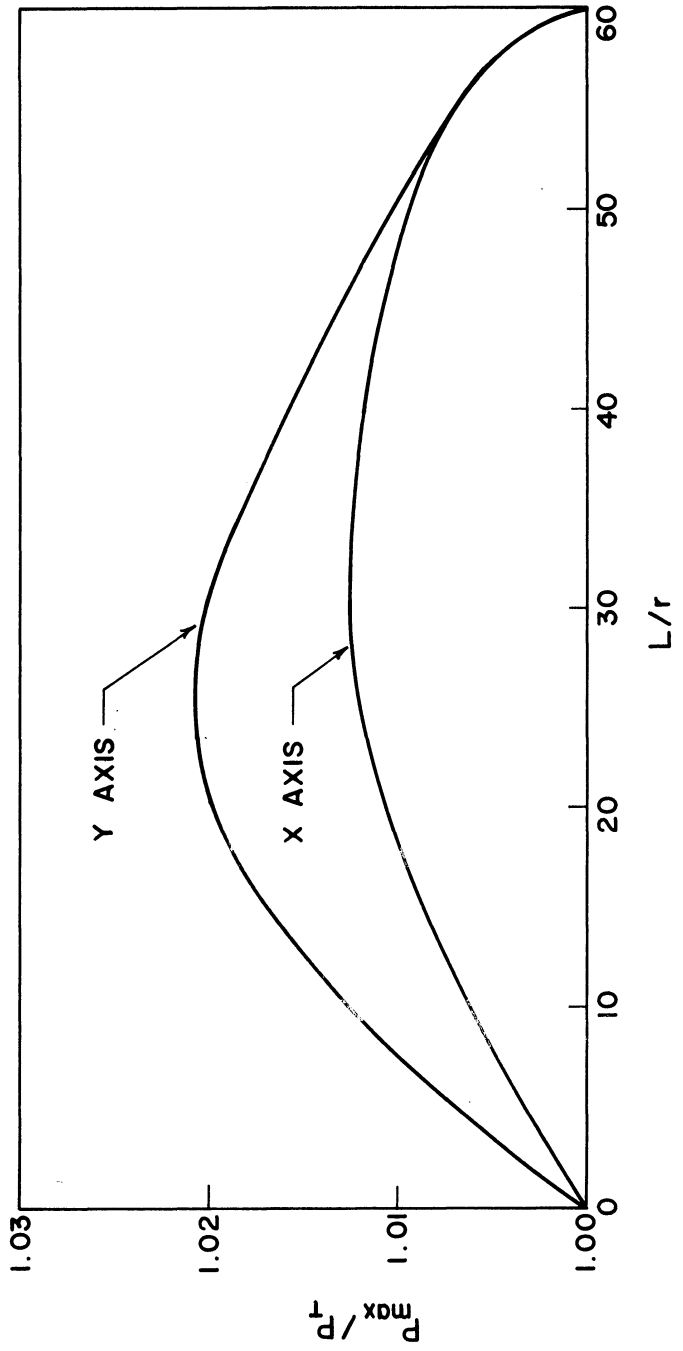

Figure 13. Increase in Load Above the Tangent Modulus Load

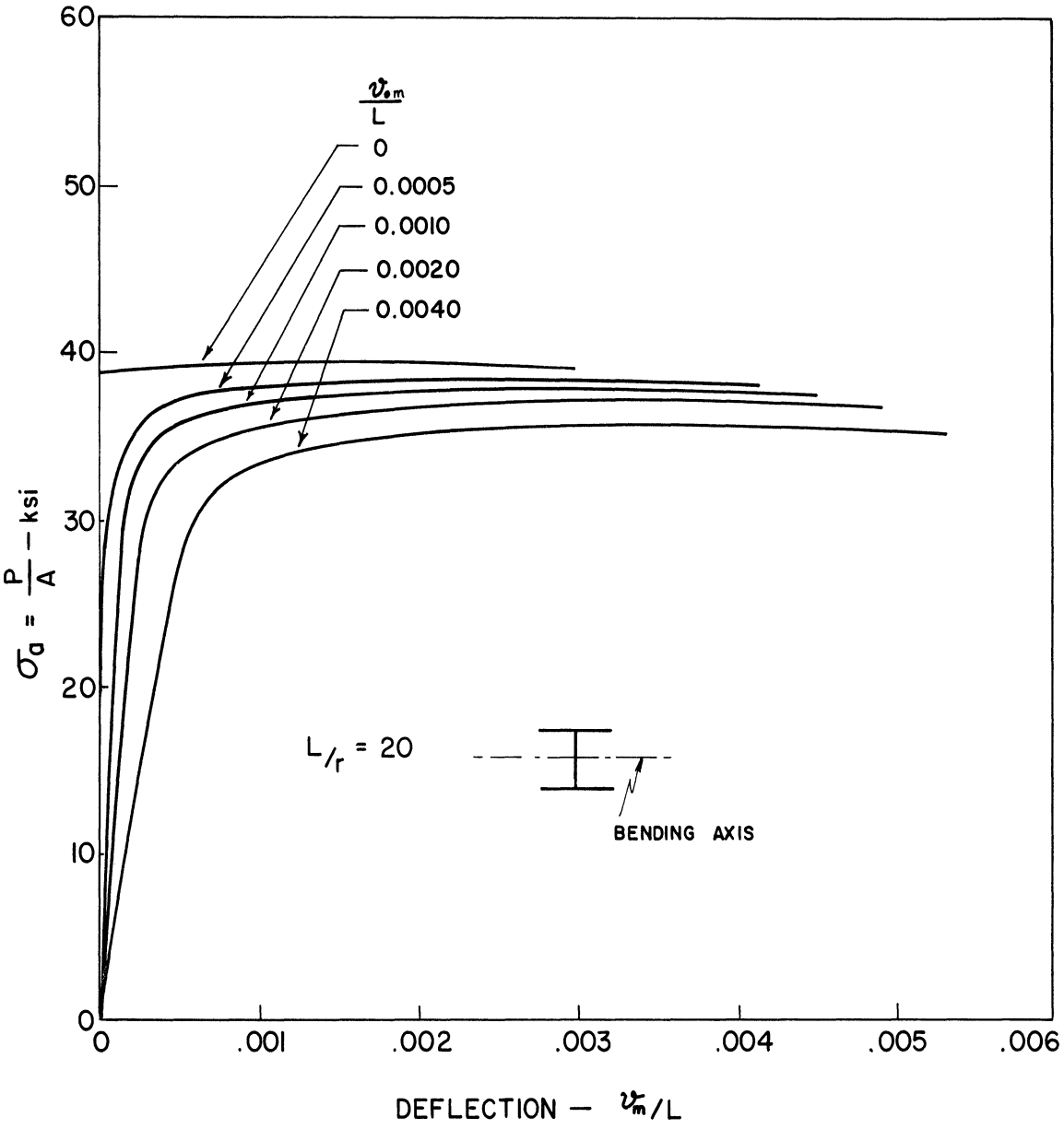

Figure 14. Load-Deflection Curves for Aluminum Alloy Columns; L/r = 20

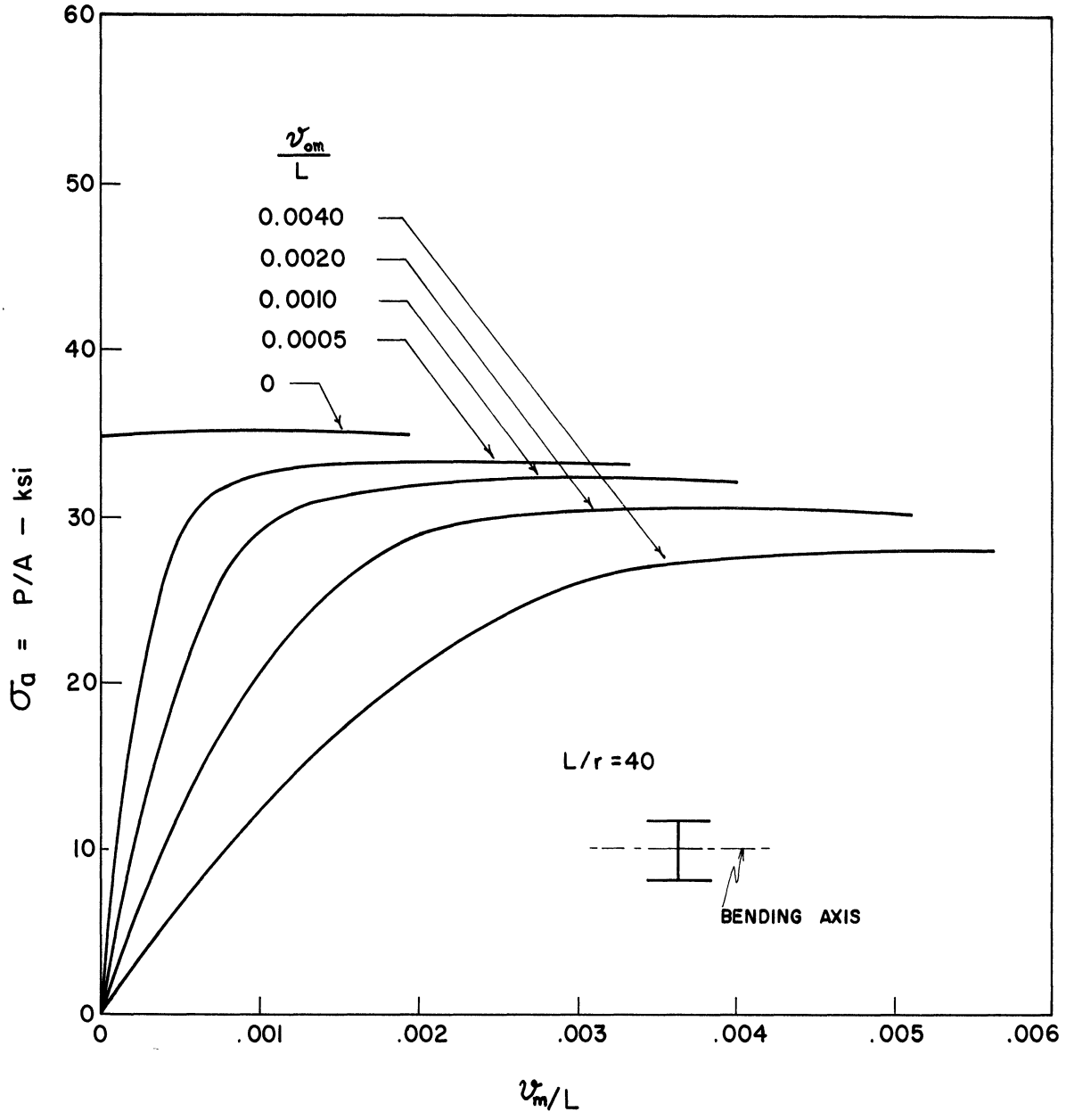

Figure 15. Load-Deflection Curves for Aluminum Alloy Columns; L/r = 40.

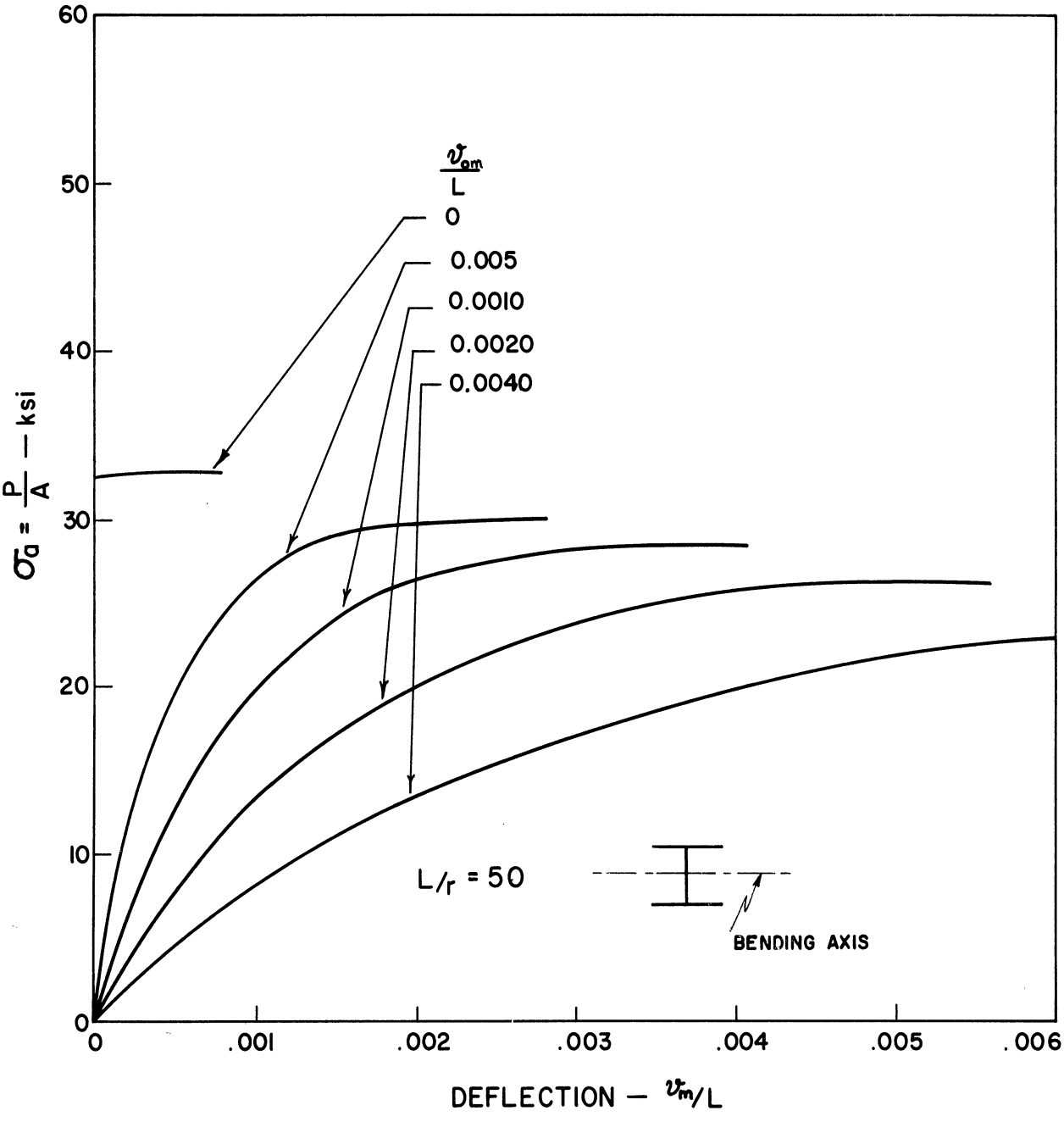

Figure 16. Load-Deflection Curves for Aluminum Alloy Columns; L/r = 50

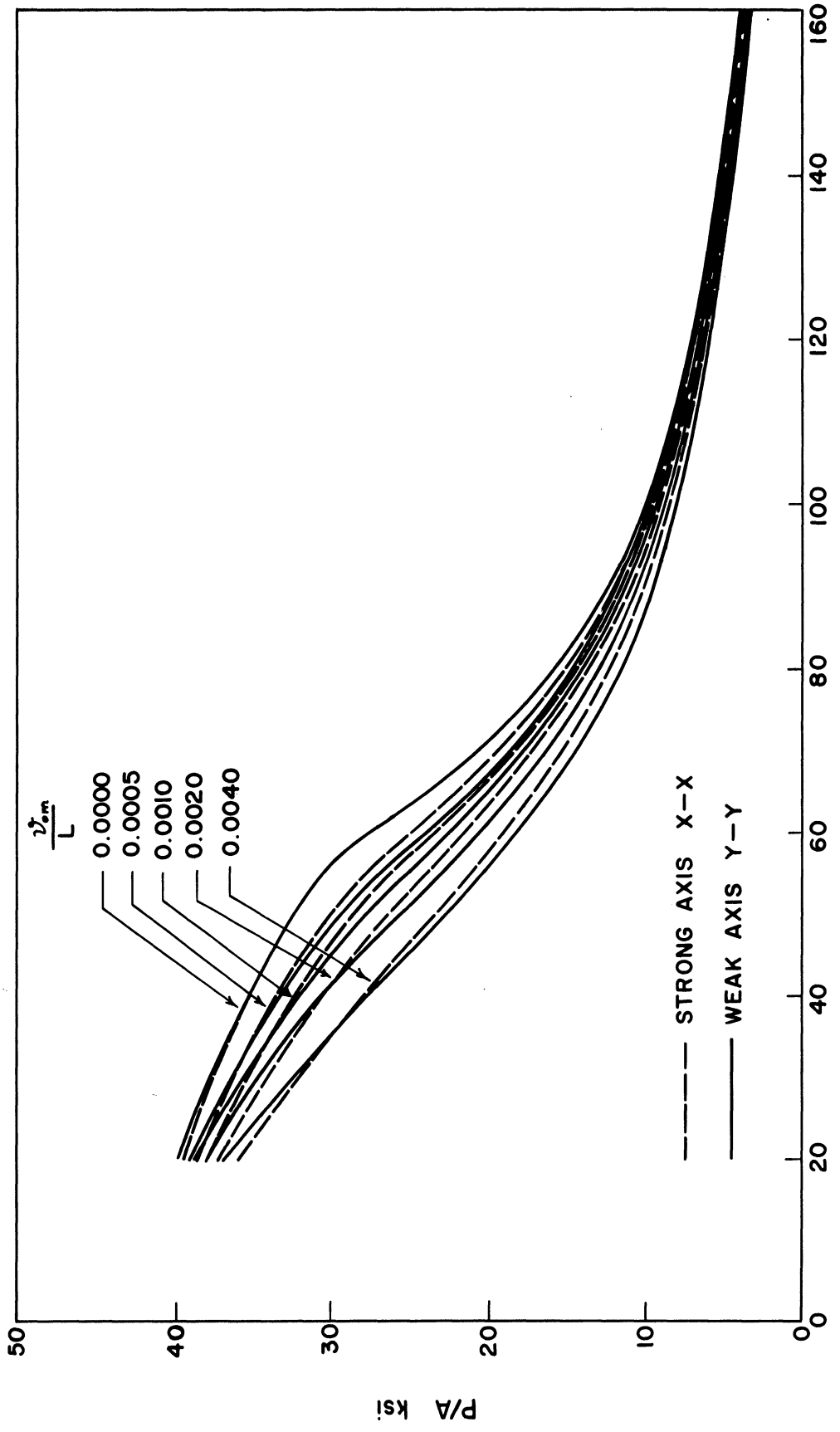

Figure 17. Aluminum Alloy Column Strength Curves

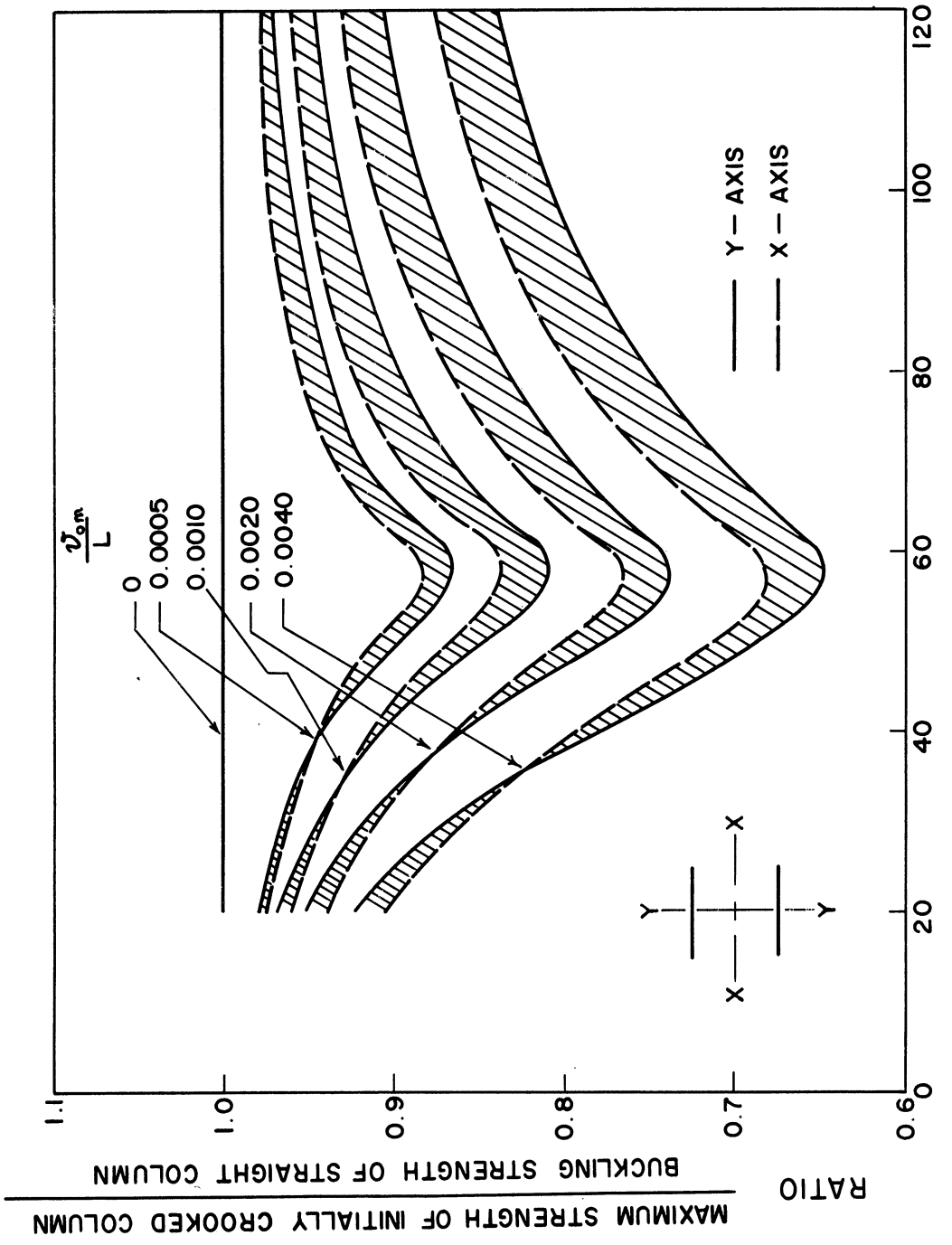

Figure 18. Comparative Strength Reduction in Aluminum Alloy Columns Due to Initial Curvature

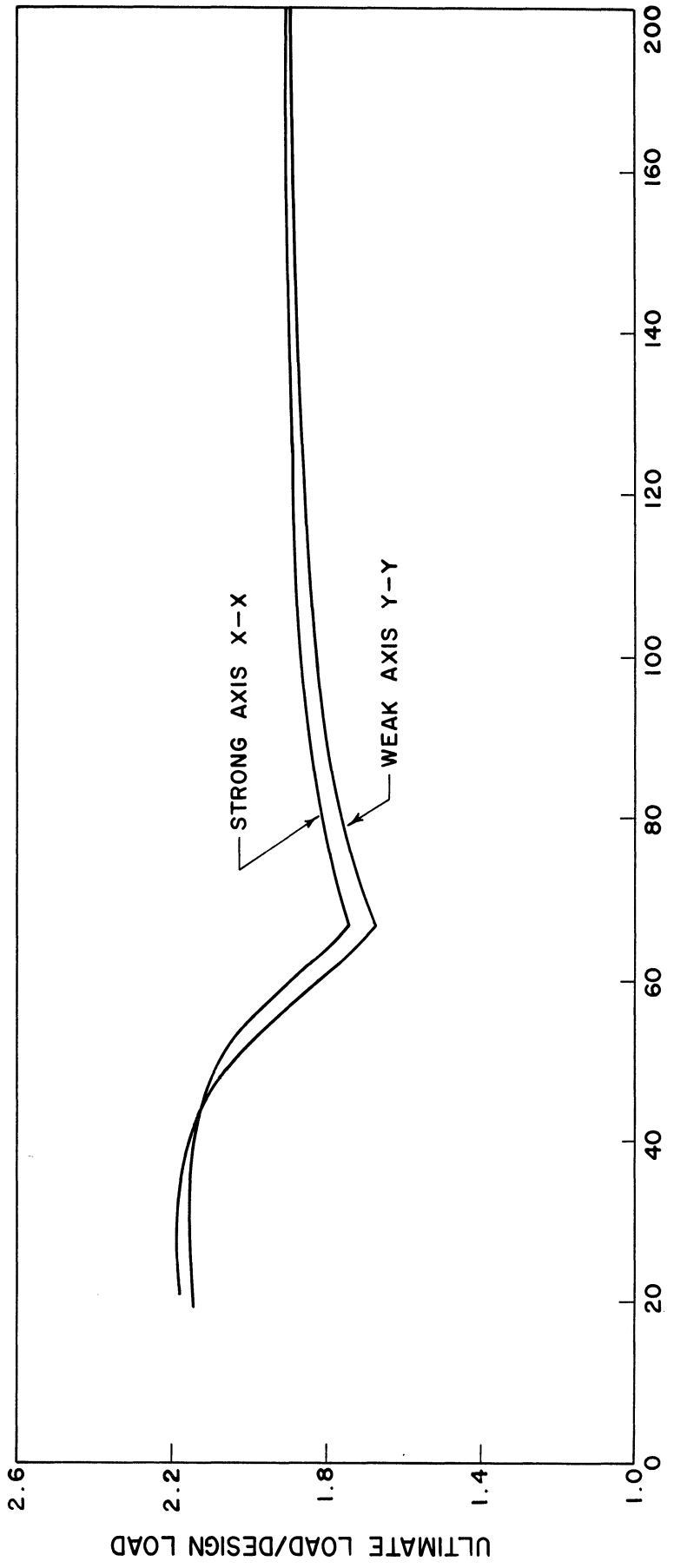

Figure 19. Design Load Factor for Wide Flange Shapes of Aluminum Alloy Columns with $v_o = 0.001L$

DESIGN CONSIDERATIONS FOR ALUMINUM COLUMNS

The "Suggested Specifications for Structures of Aluminum Alloys 6061-T6 and 6062-T6" (ASCE Proc. Paper No. 3341) gives the following allowable stress formula for columns used in buildings:

$$\sigma_a = \begin{cases} 20.4 - 0.135L/r \ , & \text{for } L/r \leq 67 \\ \dfrac{51{,}000}{(L/r)^2} \ , & \text{for } L/r > 67 \end{cases} \qquad (16)$$

In the inelastic region, this design formula is based on a straight-line approximation to the tangent modulus curve corresponding to minimum mechanical properties. In the elastic region, it is based on the Euler formula. The factor of safety used in its derivation was 1.95.

The straightness tolerance specified in the Alcoa Aluminum Handbook for extruded shapes having a circumscribing circle diameter of 1-1/2 inches or more, is .0125 inches times the length in feet. Assuming a deviation from straightness of .0120 x L(ft), corresponding to $v_o/L = .001$, the ratio of ultimate strength to design strength based on Equation (16) is given in Figure 19. This gives the theoretical safety factor for a pin-ended column (K = 1.0), having typical mechanical properties, as a function of slenderness ratio. The fact that the safety factor is greatest for short columns is due to the fact that there is a greater uncertainty of material strength, on which the strength of short columns is dependent, than of the elastic modulus, which governs the strength of slender columns.

The dip in safety at $L/r = 67$ reflects the sensitivity of column strength to initial crookedness in this range, a factor which was not directly considered in the development of the specification formula. In a discussion of these specifications,[3] Hartmann and Clark have pointed out that the effects of small amounts of initial crookedness or eccentricity may be offset by the use of conservative values of equivalent length factor as a basis for the specification formulas. To illustrate this, consider the hypothetical case of a column with typical material properties and ends restrained such that throughout loading up to ultimate strength the portion of the column between inflection points is always 0.9L. Assuming bending about the Y-Y axis and an initial crookedness of 0.001L, the theoretical safety factor is plotted in Figure 20, both for this case and for the case of pinned ends. Thus, for a relatively slight amount of end restraint, the actual safety factor for the given column varies from a value slightly above 2.2 in the short column range to a minimum of 1.97 at $L/r = 67$. It then increases with L/r to slightly above 2.2 at $L/r = 120$. The effect of initial crookedness in reducing the safety factor from 1.95 to 1.67 is, hence, offset if the column is restrained at the ends such that an actual K value of 0.9 is produced.

Although the easy-to-use specification design formula has been shown to be conservative for nominal amounts of crookedness and end restraint (at least for columns with typical material properties) it does not deal directly with the effect of crookedness. On the other hand, the procedure employed in this project to obtain maximum column

---

(3) "The U.S. Code" by E. C. Hartmann and J. W. Clark, Proc., Symposium on Aluminum in Structural Engineering, London, June 11-12, 1963, The Aluminum Federation, London

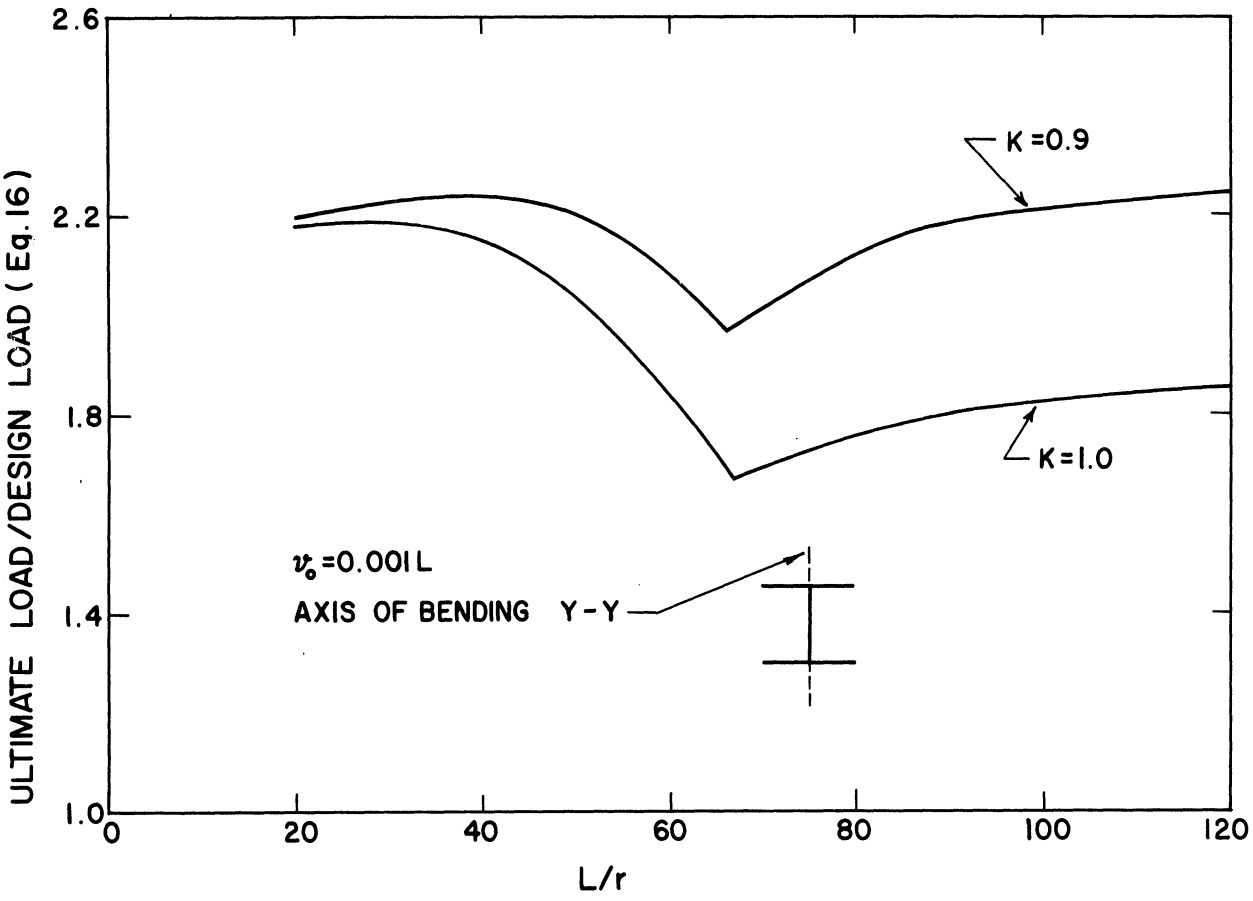

Figure 20. Comparison of Safety Factors for Columns With and Without End-Restraint

strength values does directly include the effect of crookedness, but is not easy to use for routine design use. A semi-rational interaction type formula has been considered, therefore, which includes crookedness as a factor and is relatively simple to apply. This interaction formula is:

$$\frac{\sigma_a}{\sigma_{cm}} + \frac{\sigma_a v_o c/r^2}{\sigma_b\left[1 - \left(\frac{\sigma_a}{\sigma_e}\right)\right]} \leq 1 \qquad (17)$$

where σ_a = average column stress, P/A

σ_{cm} = maximum average column stress for initially straight column

σ_b = limiting fiber stress for member subjected to bending only.

$\sigma_e = \pi^2 E/(L/r)^2$

v_o = initial crookedness parameter

c = the half-depth of the section

r = radius of gyration

The first term is the stress ratio for axial load and the second is the stress ratio for bending at the midlength of the column.

In evaluating the suitability of this relationship it was assumed that σ_{cm} was the value obtained in the simulated tests for $v_o/L = 0$, and σ_b was the 0.002 offset yield stress for the stress strain curve in Figure 7 (40 ksi) multiplied by a plastic shape factor. This shape factor was taken to be 1.5 for weak-axis bending and 1.12 for strong-axis bending of the wide flange. The corresponding values of σ_{bc} were 60 ksi and 45 ksi. Figures 21a, 21b, 22a, and 22b are each plots of three curves: the actual strength for $v_o = 0(\sigma_{cm})$, the actual strength for the

amount of initial crookedness in question, and the calculated strength based on Equation 17. Figure 21 is for strong axis bending and Figure 22 is for weak axis bending. In general, the interaction equation provides excellent correlation with the actual strengths in the short and intermediate slenderness range and is slightly conservative throughout the long column range.

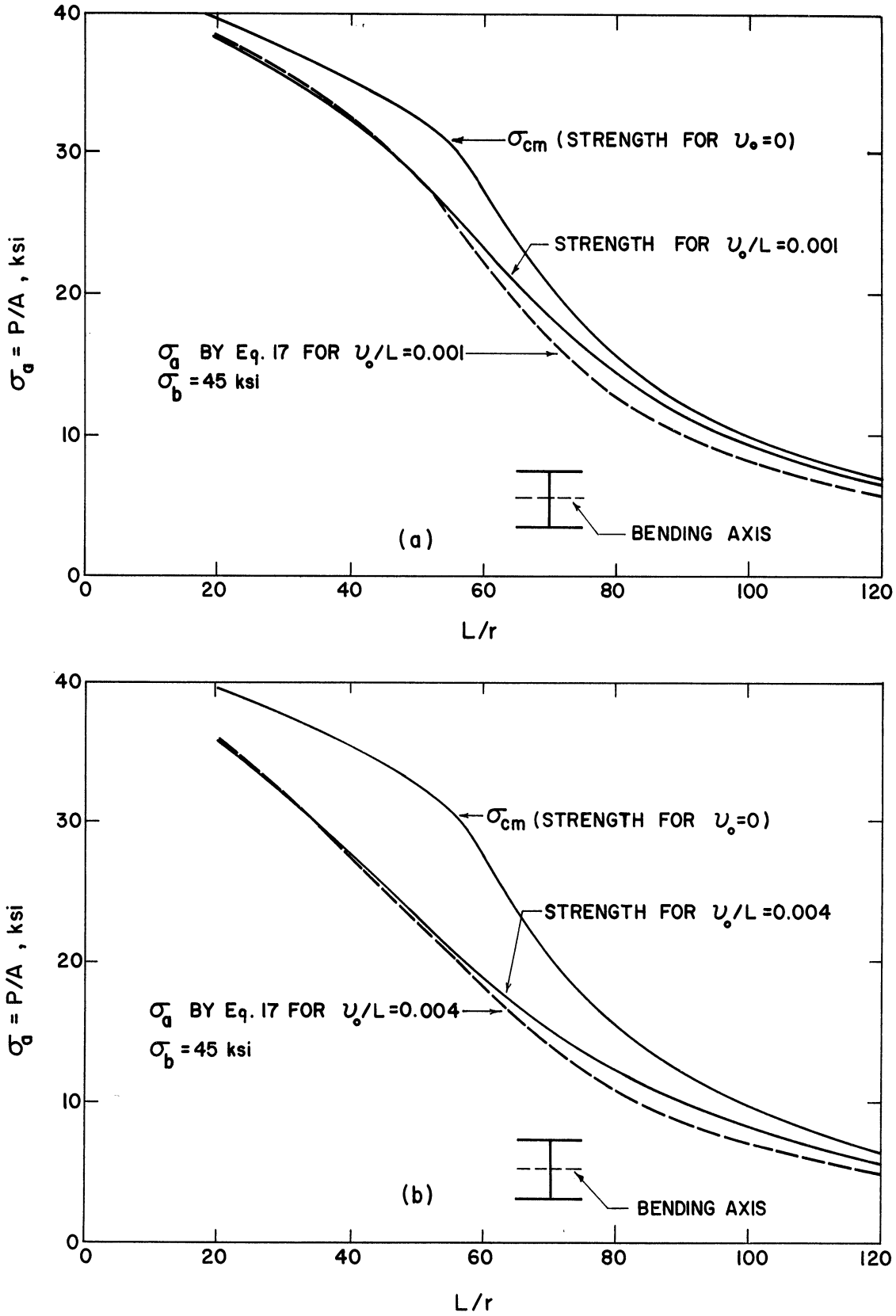

Figure 21. Comparison of σ_a by Equation 17 with Actual Strength for Strong Axis (x-x) Bending for $v_o/L = 0.001$ (Figure 21a) and $v_o/L = 0.004$ (Figure 21b)

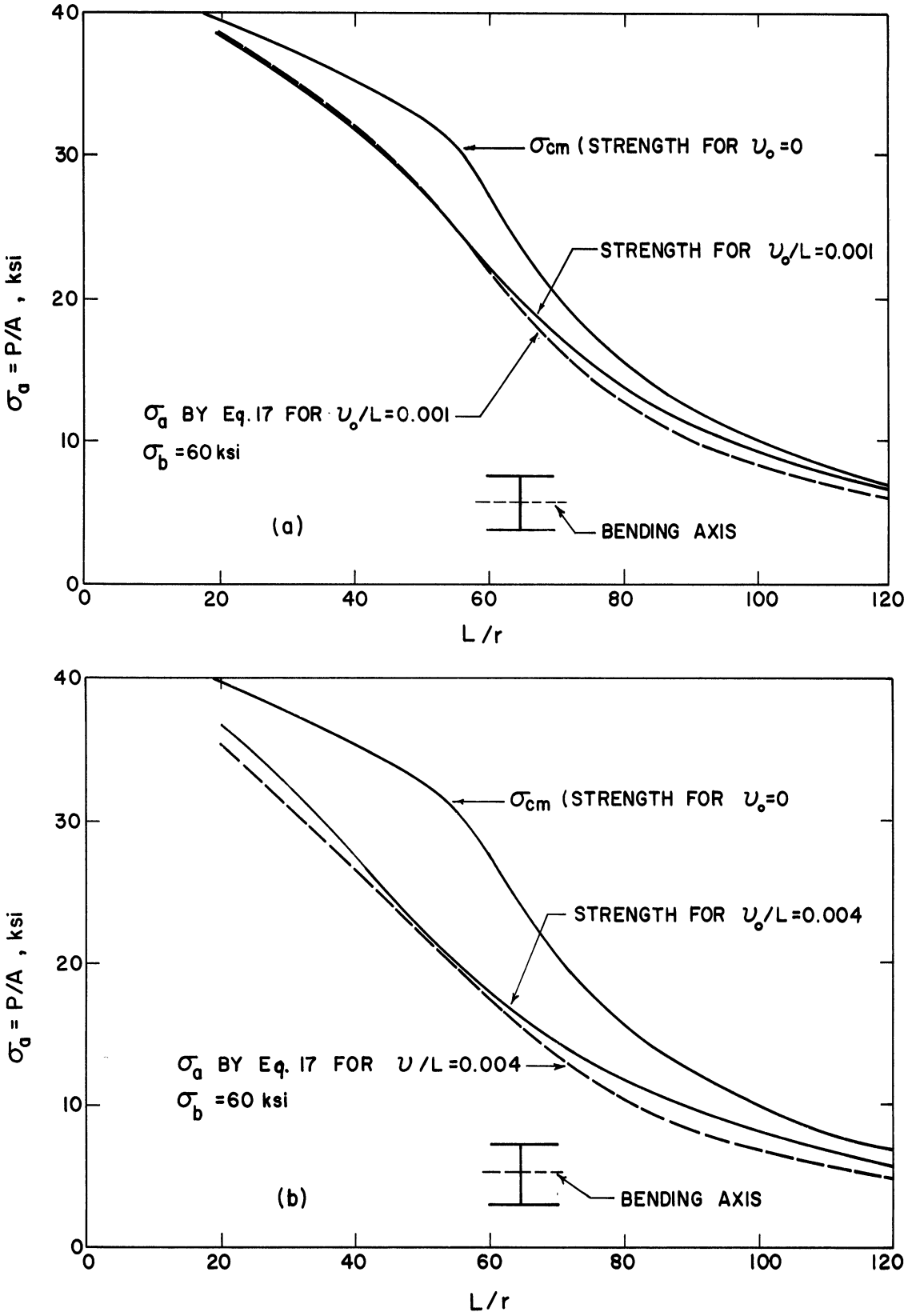

Figure 22. Comparison of σ_a by Equation 17 with Actual Strength for Weak Axis (y-y) Bending for $v_o/L = 0.001$ (Figure 22a) and $v_o/L = 0.004$ (Figure 22b)

BEHAVIOR OF STEEL COLUMNS

It will be assumed that the stress-strain diagram for steel is as shown in Figure 5a; linearly elastic up to the yield stress and thereafter perfectly plastic. If at any point within a column cross section there is strain regression after prior yield, stress reduction is assumed to be linearly elastic. The column cross-section is assumed to be that of an idealized wide flange shape in which the web is reduced to zero and thus the section consists simply of two flanges that are assumed to behave as if they were connected by a web with adequate shear capacity. Bending of the idealized wide flange shape about the weak axis is comparable to that of a simple rectangle bent about its strong axis. Bending about the strong axis is essentially the same as that of two point areas of material situated at a distance $h/2$ from the bending axis where h is the distance center to center of flange areas. Bending is considered about both the strong and weak axes.

A critical (bifurcation) load may be established if the column is initially straight and centrally loaded and if within the column cross section there exists a bisymmetric pattern of residual stress. It is assumed that compressive residual stress exists at the flange tips and that this gives way to tensile residual stresses in the remaining core sections of the flanges. The column buckling load may be theoretically determined if either (1) the distribution of residual stress is known or (2) there is available an average stress-strain diagram of a short stub column section tested as a unit and having the same residual stress pattern that is under consideration. For the idealized wide

flange shape just described the critical stress for strong-axis bending is given by Equation (2) with the $f(\eta)$ equal to η, while for weak-axis bending $f(\eta) = \eta^3$. Research into residual stress effects on steel columns was initiated by Column Research Council and a summary of the developments to date is described in Reference (1). Much of the current research has been done at Lehigh University as reviewed by Beedle and Tall[5].

In the main program of simulated tests the linear variation of residual stress in the flanges as shown in Figure 6(a) was assumed. Levels of residual stress in the program were primarily 0, 10 ksi and 20 ksi. The level of 10 ksi corresponds approximately to the $0.3\ \sigma_y$ that has been commonly accepted as an average level for structural grade steel with a yield point of 33 ksi. Recent studies at Lehigh[4] indicate that maximum residual stress levels for steels with a high yield stress are not appreciably greater than for the low yield stress steels. However, for comparative purposes, the maximum compressive residual stress level of 20 ksi was included throughout the simulated test program and in a limited number of cases the effect of a maximum residual stress level of 30 ksi was determined for the 100 ksi yield stress steel. In addition, comparative tests were made at the 10 ksi level for the parabolic residual stress pattern shown in Figure 6(b).

---

(4) Estuar, F. R., and Tall, L., "Experimental Investigation of Welded Built-up Columns", Welding Journal, Vol. 42, April, 1963.

(5) Beedle, L. S., and Tall, L., "Basic Column Strength," Trans. ASCE, Vol. 127, Part II (1962), p. 138.

In addition to the consideration of the perfectly straight column, four degrees of initial curvature were included in the test program. These included initial mid-length crookedness of L/1000 corresponding very nearly to ASTM specified allowances for sweep or camber in wide flange shapes, together with crookedness levels of half, twice, and four times this allowable value.

In summary, then, the simulated tests for weak-axis bending included the following range of parameter variation.

Steel Yield Stress	Maximum Compressive Residual Stress	Initial Crookedness	Slenderness Ratio
36 ksi 60 ksi 100 ksi	0 10 ksi 20 ksi	0 0.0005L 0.001L 0.002L 0.004L	30 40 50 60 80 100 120 160 200 240

Thus, there were 450 simulated column tests for the weak-axis bending sequences.

In strong-axis bending $f(\eta) = \eta$ and the behavior is identical with that obtainable by the aluminum column test program modified so that the effects of residual stress are used to determine an average non-linear steel stress-strain curve which is smoothly continuous above the proportional limit. With this replacement and with the web area reduced to zero the modified aluminum program was used to study the following cases of strong-axis bending in the steel column program.

Steel Yield Stress	Maximum Compressive Residual Stress	Initial Crookedness	Slenderness Ratio
36 ksi 100 ksi	0 10 ksi	0 0.001L	20 40 60 80 100 120 160 200 240

Thus, the basic program of simulated strong-axis tests of steel columns involved 72 runs.

GENERAL BEHAVIOR OF STEEL COLUMNS

The theory for buckling of steel columns with residual stress has been provided in Reference (1) and in the list of references provided therein. Figures 23, 24, and 25 illustrate the general behavior of 81 of the weak-axis bending tests of steel columns for KL/r ratios of 40, 100, and 160, respectively. The load-deflection curves are plotted for the three yield stresses and three residual stress levels but only the two largest initial crookedness ratios are included along with the curves for initially straight columns.

Since the initial crookedness was assumed to be distributed as a half-sine wave, the maximum center deflection is given by the simple amplification formula so long as the column remains completely elastic.

$$v_m = \frac{v_{om}}{\left(1 - \frac{P}{P_e}\right)} \tag{18}$$

In Equation (18) the plotted deflection <u>includes</u> the initial crookedness and is equal to $v_m + v_{om}$. In all three of the figures, dots interjected at various points along the common stem indicate loads and deflection at which the maximum stress (including the residual stress as well as that caused by bending moment plus axial load) equals the yield point. At these points the various curves start to diverge from the common stem but this is not always immediately observable on the curves. For the idealized situation wherein the column is initially straight, the load-deflection curves show no deflection until one of three loads is reached:

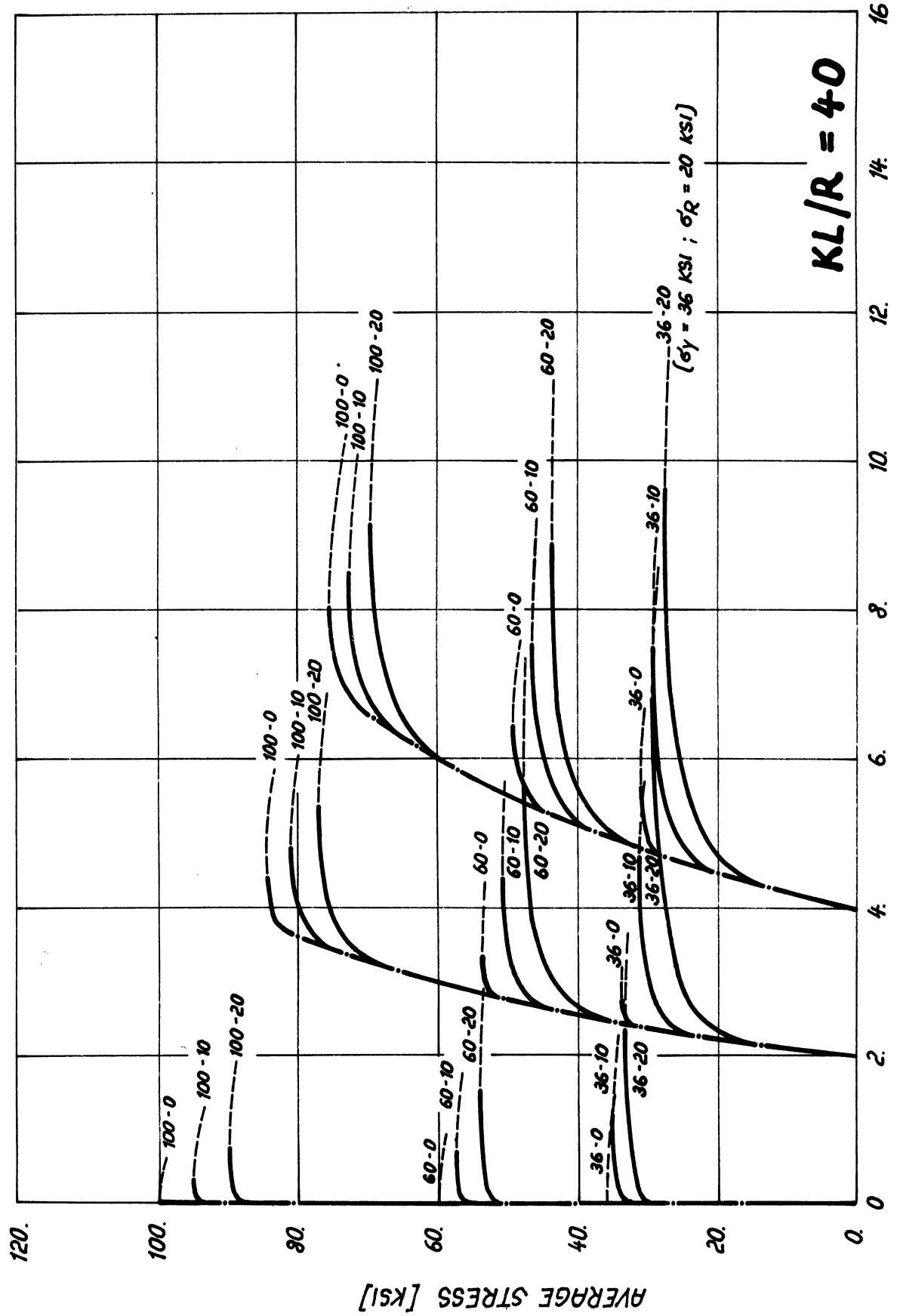

Figure 23. Load Deflection Curves for WF Steel Columns, Weak-Axis Bending, KL/r = 40

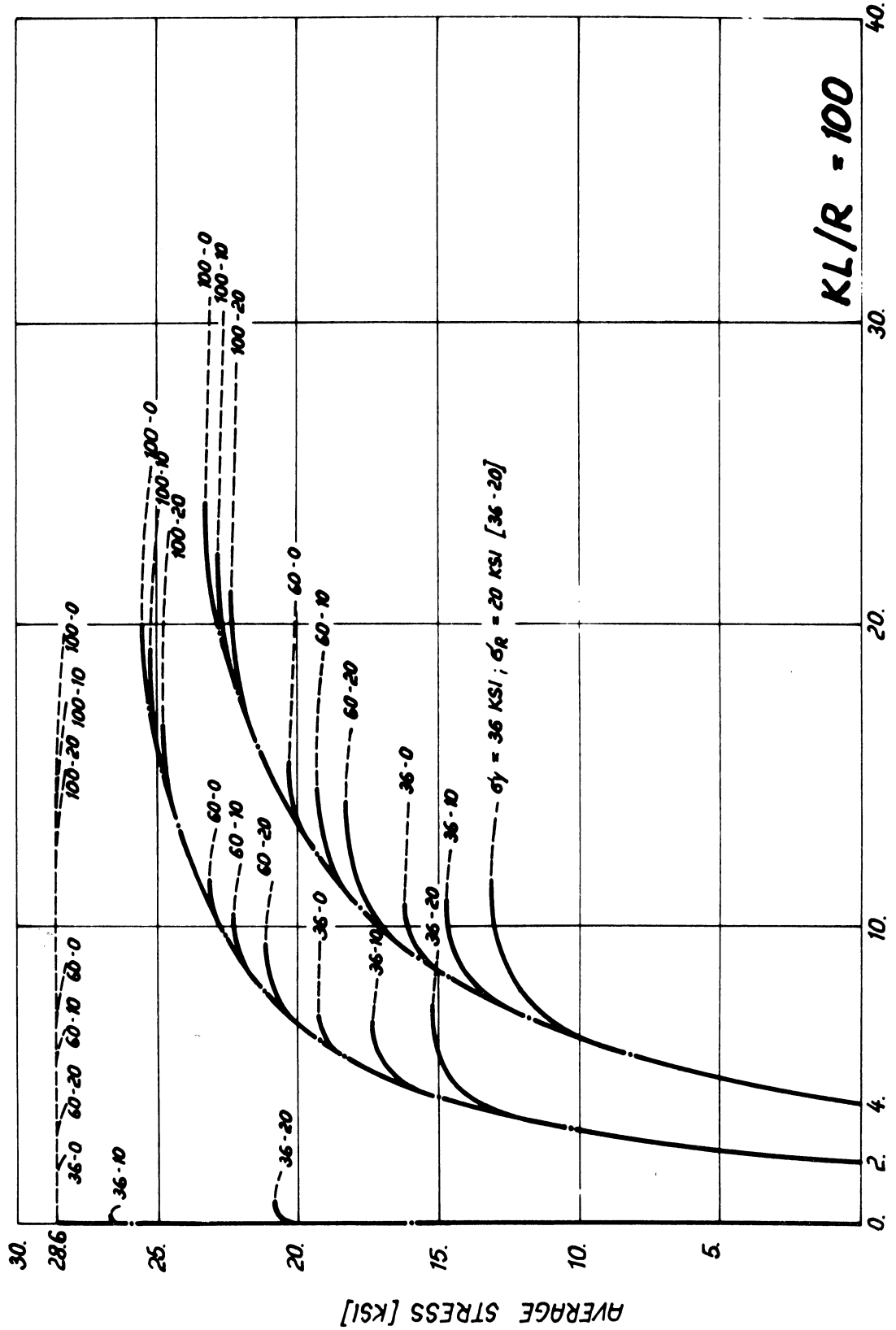

Figure 24. Load Deflection Curves for WF Steel Columns, Weak-Axis Bending, KL/r = 100

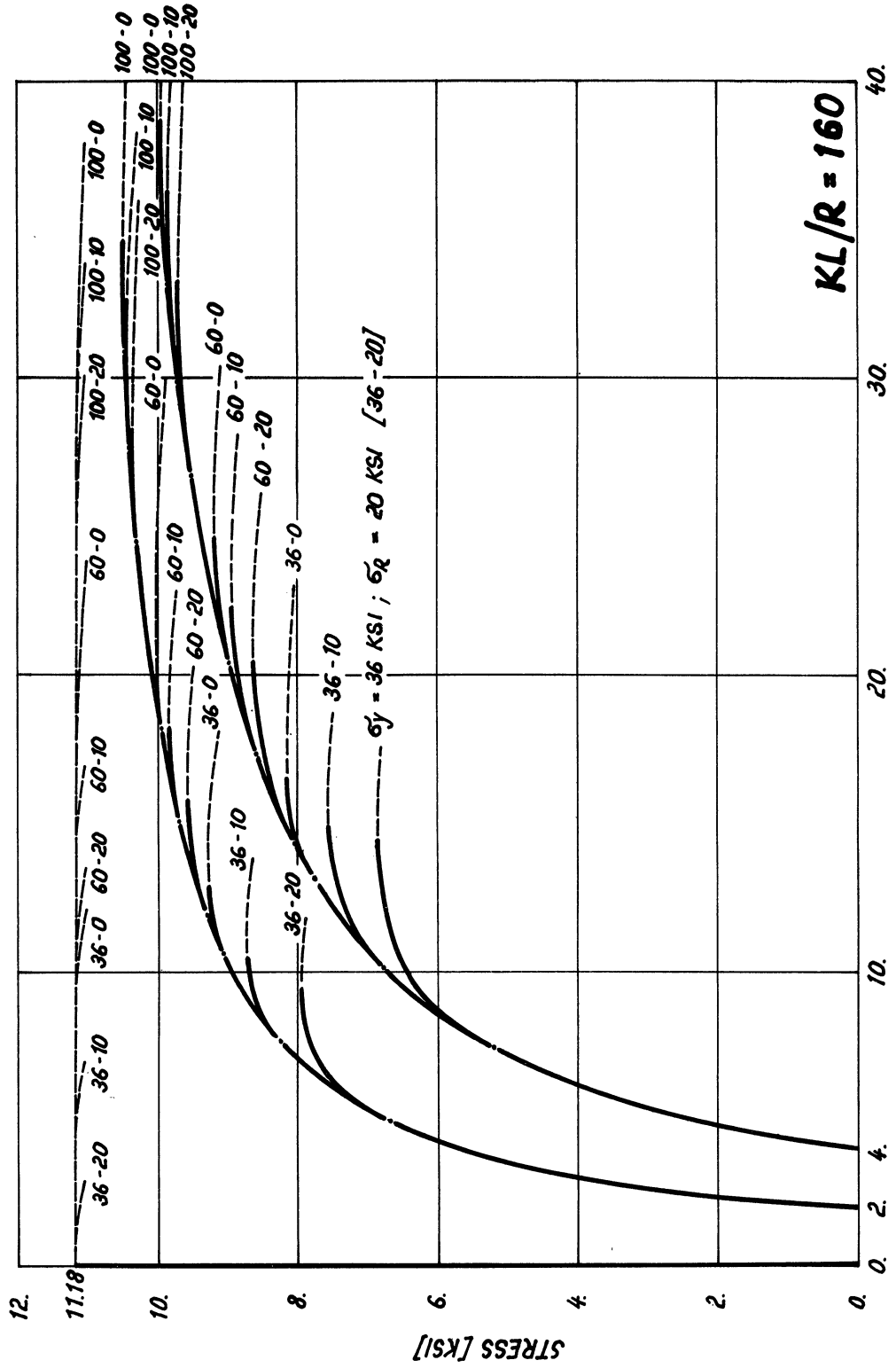

Figure 25. Load Deflection Curves for WF Steel Columns, Weak-Axis Bending, KL/r = 160

(1) The yield point load for the case of zero residual stress in short columns with $\frac{L}{r} < \pi\sqrt{\frac{\sigma_y}{E}}$.

(2) The Euler buckling load for slender columns, having $\frac{L}{r} > \pi\sqrt{\frac{\sigma_y - \sigma_{RC}}{e}}$ where σ_{RC} is the maximum residual stress in compression.

(3) The critical inelastic buckling load by Equation (2) with $f(\eta) = \eta^3$ for those columns which buckle in the inelastic range about the yy (web) axis.

Considering now Figure 23 for KL/r = 40 , which is typical of the large bulk of columns actually used in heavy structures, the average column stress reaches the yield stress in all cases for which $v_o = 0$ and there is a fairly rapid decline from maximum load at small deflections.

In Figure 24 the slenderness ratio is at the upper end of the usual design range. In this case all but two of the initially straight columns reach the Euler stress of 28.6 ksi. For the initially curved columns the greater effect of residual stress in comparison with KL/r = 40 may be noted. Referring to Figure 25, for KL/r = 160 , it is to be noted that all of the initially straight columns reach the Euler buckling stress of 11.18 ksi. It is of interest that these columns maintain this load for much greater deflection than at KL/r of 100 and that the Euler load is maintained for increased deflections in the case of higher yield stresses. Thus, though there is no difference in the buckling load of slender steel columns, there may be applications where the ability of the higher yield stress material to absorb large deflections without inelastic behavior is of some advantage.

Figures 26 and 27 show the maximum column strength curves, with and without the effects of residual stress and initial crookedness (alone or in combination and at levels usually considered proper as a basis for design) for both weak-axis and strong-axis bending, respectively. Also shown in each of these figures is a plot of what has become known as the "CRC column strength curve", accepted in 1961 as a basis for the current AISC Specification formulas[6], together with a normalized plot of the AISC design formula for centrally loaded columns. The good agreement between AISC design practice and the maximum strength of A36 columns which have nominal amounts of initial crookedness as well as residual stress is brought about by the variable factor of safety that increases with increasing slenderness and reaches a maximum value at $\lambda = \sqrt{2}$.

Only the column strength curves associated with yield stresses of 36 and 100 ksi have been plotted. Residual stress, when included, is held at a constant level of 10 ksi maximum and thus is very nearly equal to $0.3\ \sigma_y$ for structural carbon steel but only 10 per cent of the yield stress for high-strength steel. Column strengths (reduced by effects of initial crookedness and residual stress) in comparison with idealized strengths (with these adverse factors absent) show that the maximum effect of either factor, alone or in combination, always occurs when the dimensionless slenderness ratio parameter λ equals unity. It is also

---

(6) Manual of Steel Construction, Sixth Ed., American Institute of Steel Construction, 1963.

seen that the effect of initial curvature, for a given residual stress magnitude, is greatest at the point where the curve for residual stress alone meets the Euler curve. For values of λ greater than this Euler intersection point, the effects of initial curvature gradually diminish. Figures 26 and 27 also show that, when residual stress is held at a constant level, no single non-dimensionalized curve is satisfactory for different levels of yield stress. These curves also show that the basic CRC strength formula is satisfactory for higher strength steels for columns with nominal levels of combined crookedness and residual stress.

In Figure 28 are plotted the ratios obtained by dividing the strength of steel columns having nominal imperfections (alone or in combination) by the idealized strengths of a perfect column, that is, one with neither residual stress or initial crookedness. The strength of such a perfect column is the full yield load for L/r less than $\pi\sqrt{E/\sigma_y}$ and is the Euler load for L/r greater than $\pi\sqrt{E/\sigma_y}$. Figure 28 shows that the separate strength reductions caused by initial crookedness alone or by initial residual stress alone cannot be added to yield an approximation of the strength reduction due to crookedness and residual stress in combination. Figure 28 is based on weak-axis bending but the curves for strong-axis bending are similar.

The curves A show the effects of residual stress alone, i.e., no effect if the Euler load is reached below the effective proportional limit of the steel. Curves B show the effect of initial crookedness

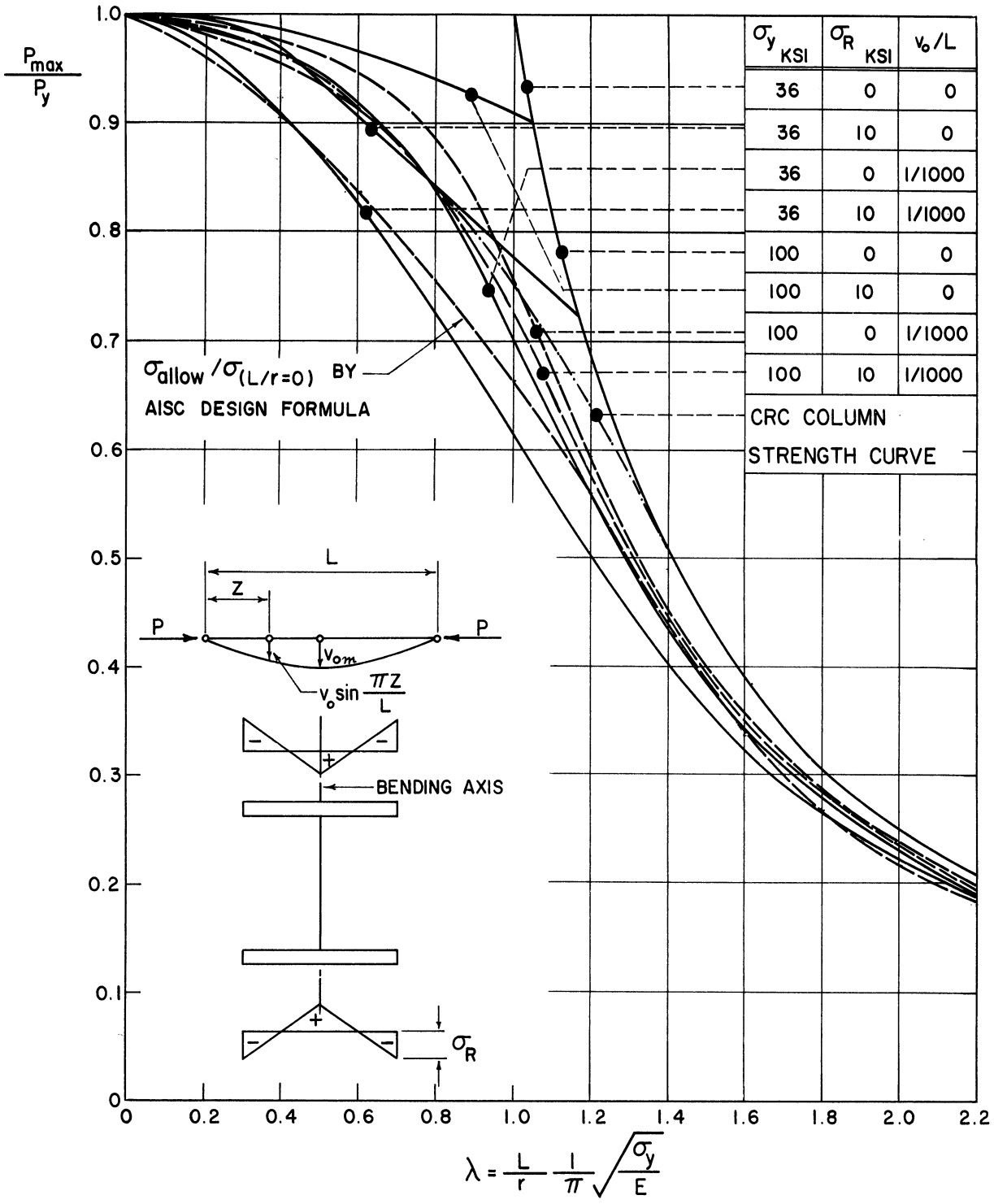

Figure 26. Column Strength Curves for Weak-Axis Bending of WF Steel Shapes

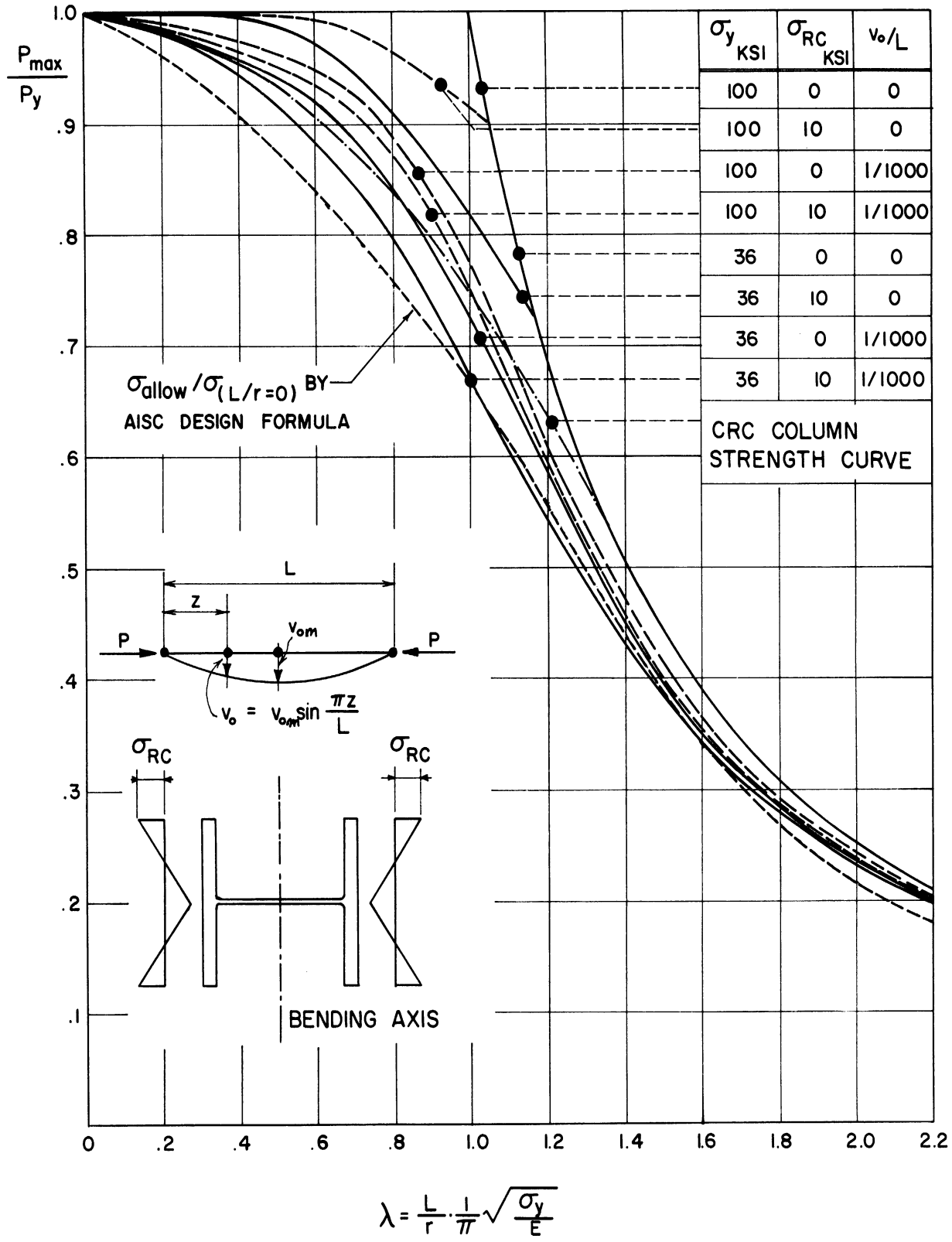

Figure 27. Column Strength Curves for Strong-Axis Bending of WF Steel Shapes

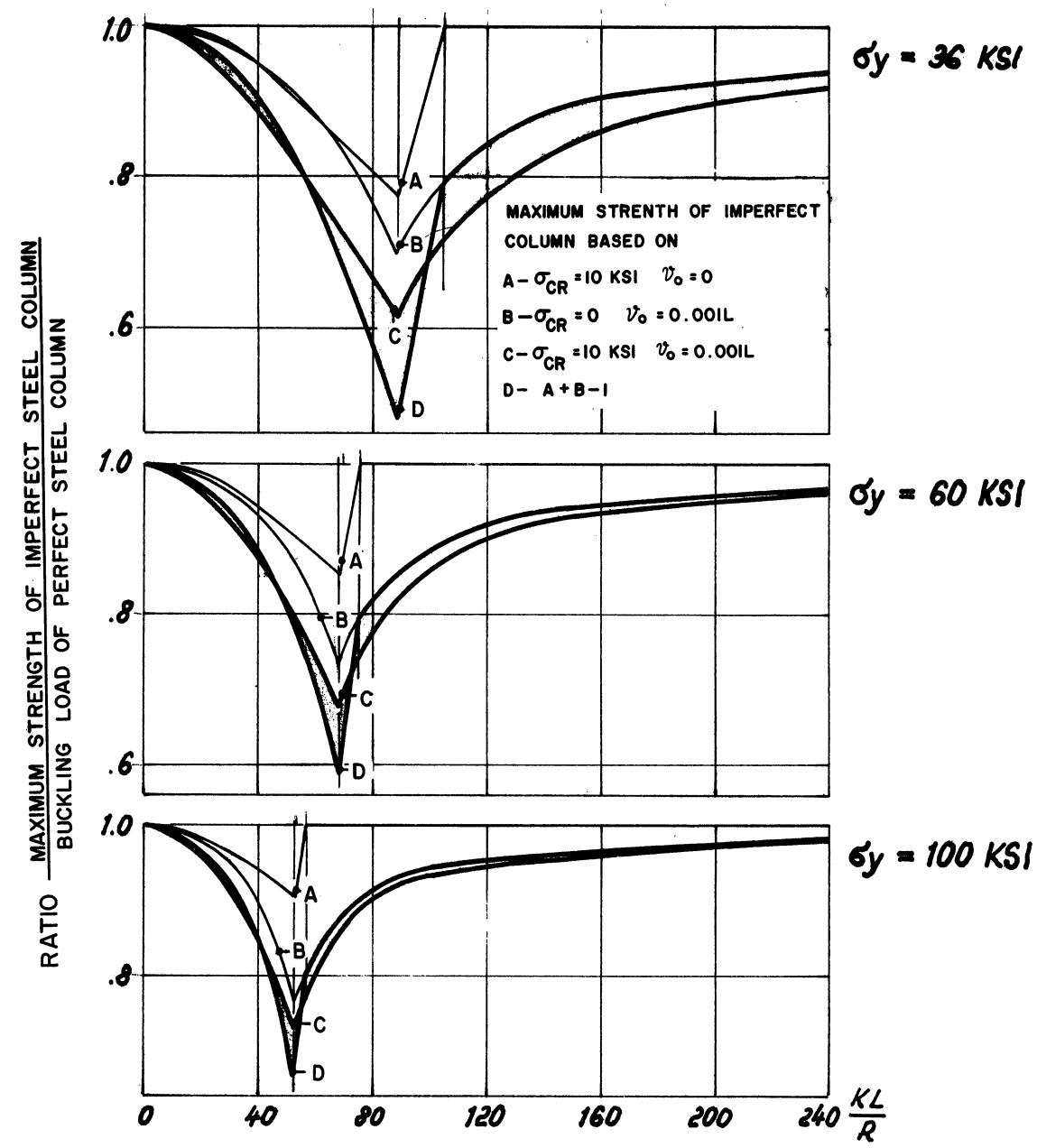

Figure 28. Ratio $\frac{\text{Maximum Strength of Imperfect Steel Column}}{\text{Buckling Load of "Perfect" Steel Column}}$ in Weak-Axis Bending, for Various Combinations of Nominal Residual Stress and Crookedness

alone. The separate effects of initial crookedness and residual stress each reach a maximum when $L/r = \pi \sqrt{E/\sigma_y}$. Curve C shows the maximum strength obtained in the simulated column tests when initial crookedness and residual stress are in combination, whereas Curves D represent column strength estimates obtained by subtracting the sum of the reductions due to the separate effects from the strength of a perfect column. In the vicinity of $L/r = \pi\sqrt{E\ \sigma_y}$, Curves C are above corresponding Curves D but for L/r less than about two-thirds of $\pi \sqrt{E/\sigma_y}$ there is fairly good agreement. For slender columns, Curves C fall below corresponding Curves D. This is due to the fact that while the Euler buckling load of a straight column below the effective proportional limit is not affected by residual stress, the bending resistance is eventually reduced by residual stress regardless of slenderness ratio.

A comprehensive summary of the bulk of the weak-axis tests is provided by Figure 29 for each of the three yield stresses. The ordinates are ratios of average axial stress at maximum load divided by the yield stress. The abscissae are the amounts of initial crookedness. Thus, by use of these curves, one can estimate the maximum column strength for any combination of initial crookedness, yield stress, residual stress, and slenderness rates. These curves again show the degree to which increasing slenderness ratio and/or increasing yield stress tend to reduce the effects of initial crookedness. It also may be noted that for the short columns residual stress has roughly similar strength-reducing properties at various yield stresses but that for the more slender columns the effect of residual stress is almost negligible for higher strength steels. For these higher strength steels the initial crookedness is more important than residual stress.

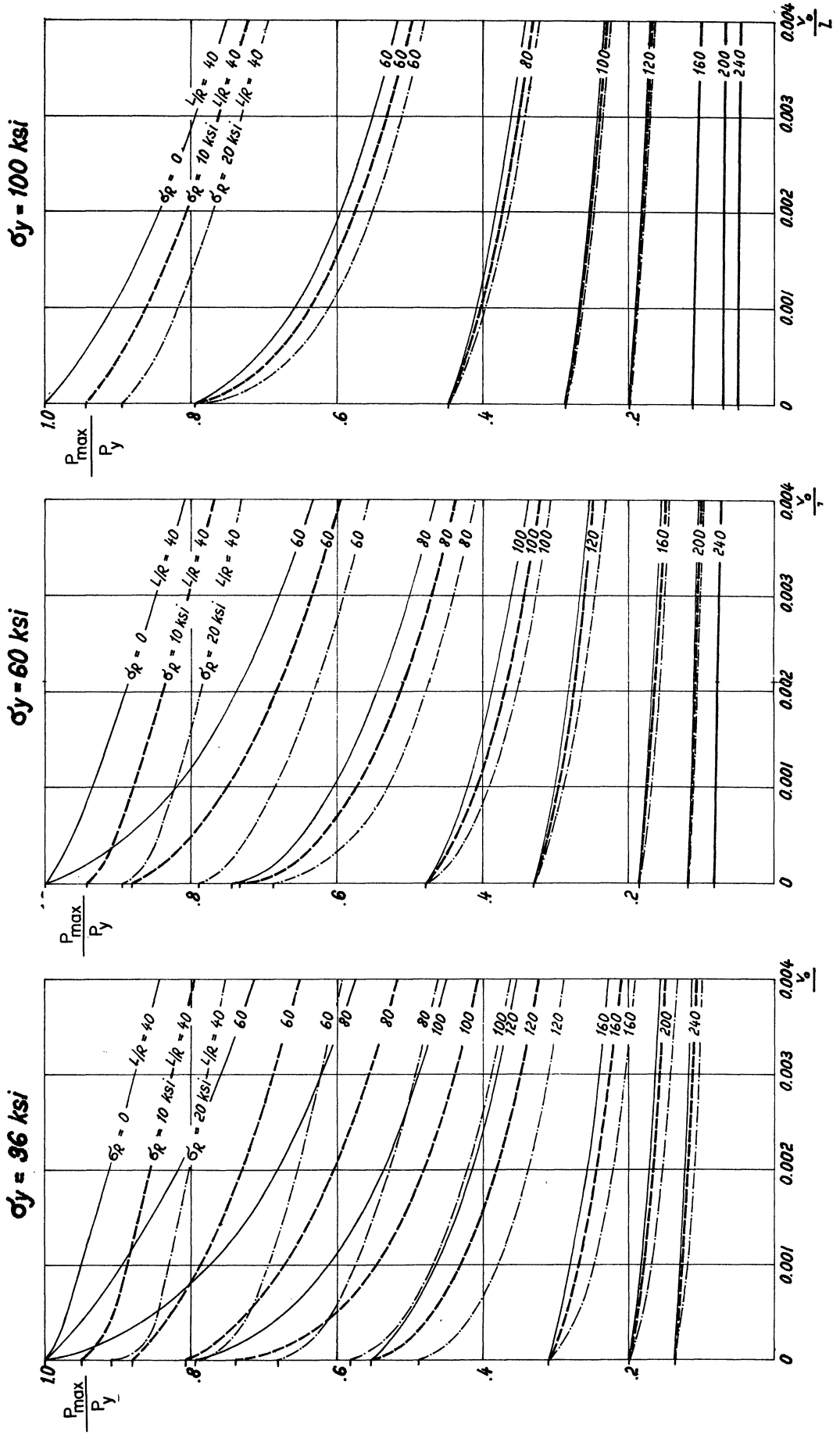

Figure 29. Summary of Maximum Strengths of Steel Columns (Weak-Axis Bending).

Figure 30 shows the development with increasing load of the stress distribution patterns in the flanges at different locations along a short steel column ($KL/r = 40$). At increments $L/8$ from the center of the column to the end, stress distribution development is shown for the initially straight column, the slightly crooked column, and the column with a large amount of initial crookedness. The flange edges on one side of the column with the large amount of initial crookedness never reach the yield stress level. In all three cases, as the maximum column load is approached, the increase in load comes about very largely from the increased amount of plastified material in the concave side of the column. The increments of bending moment that must accompany increments of load are largely elastic and are in the convex half of the column section.

MISCELLANEOUS CONSIDERATIONS IN STEEL COLUMNS

Three different special studies are now considered. All pertain to weak-axis bending of wide flange shapes. (1) The relation between load at initial yield and maximum column strength; (2) The effect of assuming a nonchanging column deflection shape in the yield range; and (3) A comparison between two different patterns of residual stress across the column flanges. All three of these special studies are summarized in Figure 31.

Initial Yielding in Relation to Maximum Column Strength

Referring to Figure 31, Curve 1 represents the load at initial yield if the column is perfectly straight whereas Curves 4 or 6 give the maximum strength of an initially straight column for two different patterns of residual stress. When both the residual stress and initial crookedness are present, the same comparison of residual stress patterns is provided by Curve 2 for load at initial yield and curves 5 and 7 for maximum strength.

The more realistic situation involving both initial crookedness and residual stress in combination shows by the comparison between Curves 2 and either 5 or 7 that the load at initial yield is appreciably below the maximum column strength for all usual design slenderness ratios. The reduction amounts to about 10 per cent for $KL/r = 120$ and increases with decreasing KL/r .

Effect of Change in Deflected Shape of the Column in the Inelastic Range

In order to simplify beam-column studies in the inelastic range

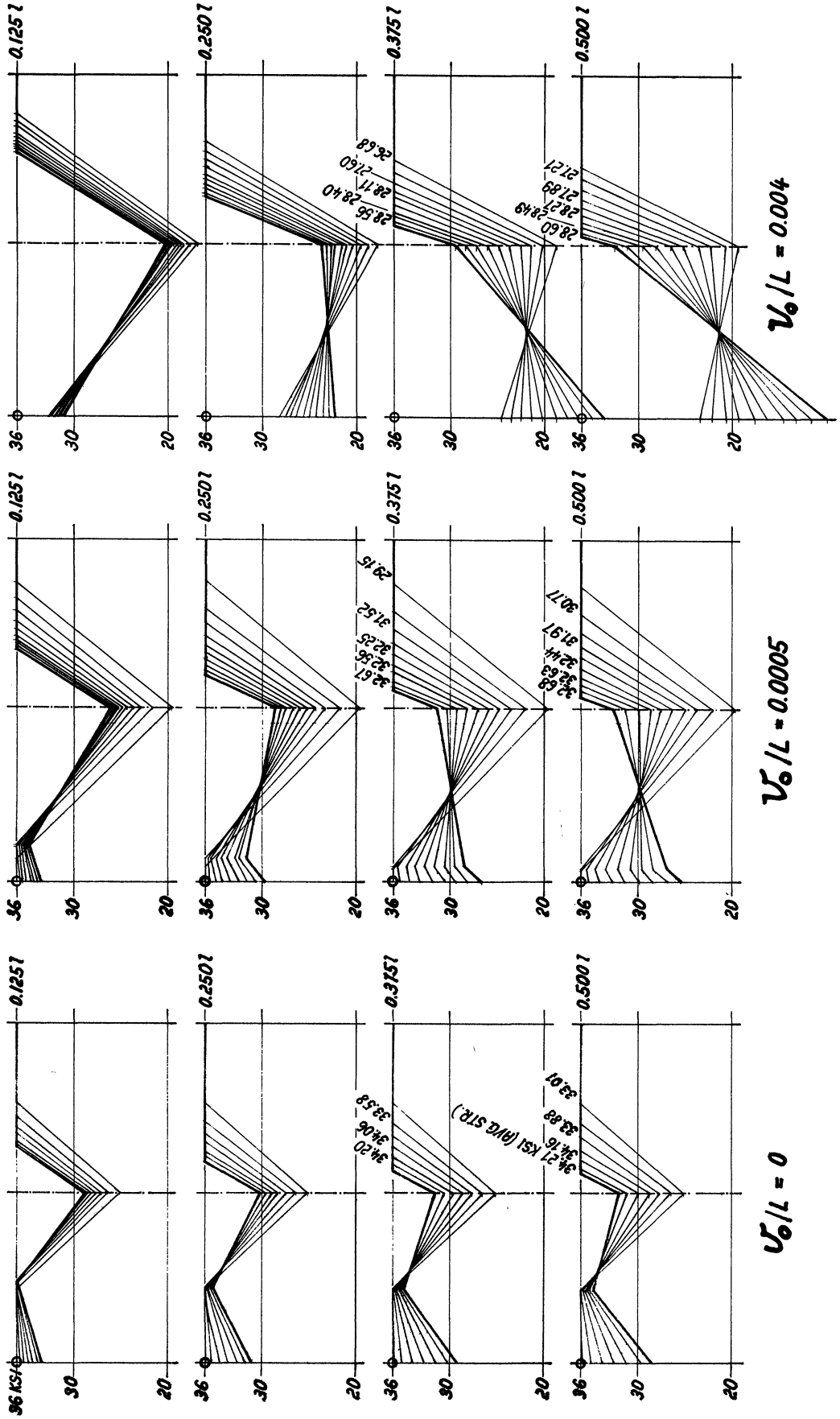

Figure 30. Stress Distribution Patterns in Flanges at Different Locations and Loads of Short $\frac{L}{r} = 40$ Steel Columns with Different Initial Crookedness

of behavior it is frequently assumed that the column deflection curve remains unchanged throughout the inelastic range. It is commonly assumed to remain a sine curve. In the present investigation a sine curve was assumed for initial crookedness, but the actual shape of the column was determined iteratively at each increment of load in the inelastic range. In Curve 3 of Figure 31, however, the deflection (computerwise) was held as a sine curve throughout the inelastic range of behavior. Curve 5 is from the regular simulated test program for the same values of σ_y , residual stress, and initial crookedness. The maximum strengths are slightly greater by Curve 5 than by Curve 3. No general conclusions can be drawn since this comparison was made for only nominal amounts of residual stress and initial crookedness.

Effect of Differences in Initial Residual Stress Pattern

The initial residual stress patterns in the flanges of wide flange shapes which are allowed to air cool after rolling have been shown usually to be between the straight line and parabolic distributions illustrated in Figure 31. Curve 4 for an initially straight column with the straight line residual stress pattern should be compared with Curve 6 for the parabolic initial residual stress distribution. Curve 5 should be similarly compared with Curve 7 for columns with a nominal degree of initial crookedness. It is seen that when both initial crookedness and residual stress are present, the differenct between patterns of residual stress causes less effect on column strength than when columns are initially straight.

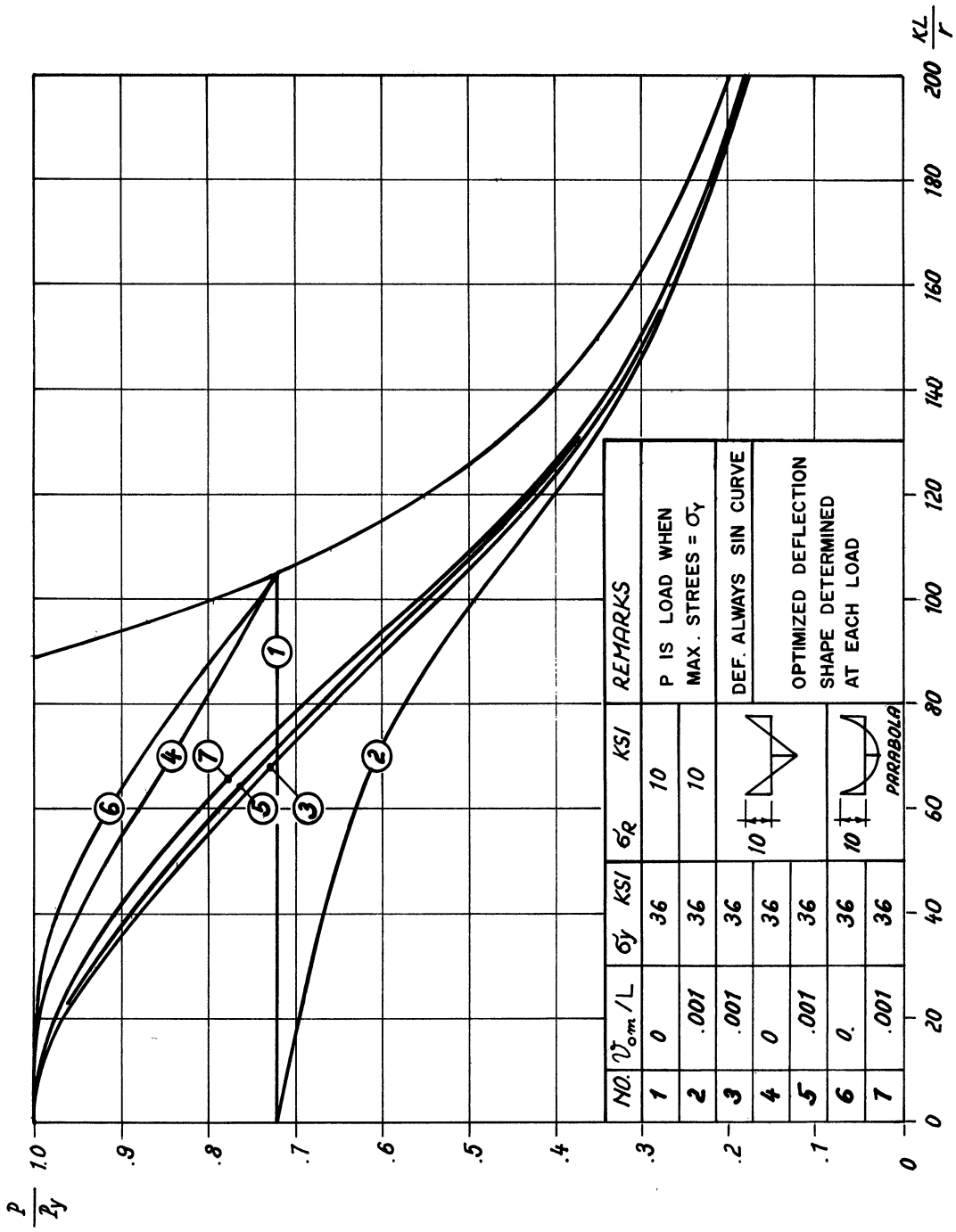

Figure 31. Miscellaneous Effects of Computational Procedure as to Deflected Shape, Residual Stress Distribution, and Relation Between Initial Yield and Maximum Column Strength

DESIGN CONSIDERATIONS FOR STEEL COLUMNS

The design of nonferrous columns has usually been based on the assumption that they were initially straight and that the strength could be predicted by the tangent modulus formula. In the design of steel structures, particularly railway and highway bridges, the basic principle of design has been the calculation of the load at which the maximum column stress, including that caused by bending moment and including an allowance for initial curvature and/or eccentricity, reaches the yield point. The average column load when this occurs is then divided by a factor of safety to yield a safe design load. When bending moment is due only to accidental eccentricity or curvature in a nominally straight column, the rather cumbersome secant or other similar formula is replaced by the simple parabolic reduction formula, of the following type:

$$\sigma_a = A - B\left(\frac{KL}{r}\right)^2 \qquad (20)$$

Any nonlinearities in stress-strain behavior due to the presence of residual stress or other causes are ignored. This procedure is currently followed in AREA and AASHO design specifications.

In applications to building construction, recommendations of Column Research Council have been followed, resulting in a modified critical load approach based on Equation (2), but approximating the average between strong and weak-axis buckling of wide flange steel columns. This procedure ignores effects of accidental curvature but takes account of the effect of nonlinearity in the average stress-strain curve that is introduced by the presence of initial residual stress. Paradoxically,

either one of these approaches may be used to give essentially the same design results since either the effects of residual stress alone or the effects of end eccentricity or initial curvature alone may be arbitrarily exaggerated to compensate for the fact that in any real column, both effects are present.

The present investigation provides a basis for the dual consideration of both initial crookedness and residual stress in the development of improved design formulas.

In Figure 32 are plotted curves in which the load at first yield in a column free of residual stress is divided by the maximum computed column strength based on both crookedness and residual stress. Thus the maximum stress design procedure (ignoring residual stress) would be unconservative when the ordinate is greater than unity. Although a rather complete range is covered in Figure 32, the following discussion will be based largely on the nominal values of initial curvature of 0.001L and maximum residual compressive stress of 10 ksi. Thus, for all nominal levels of residual stress combined with accidental crookedness, regardless of steel yield stress, the maximum stress design approach is never unconservative by more than about 10 per cent. As initial crookedness increases, the estimates by the maximum stress theory tend to become more conservative but are never overconservative by more than a few per cent when the residual stress is equal to 10 ksi. It should be noted that if residual stresses are present to a greater amount than 10 ksi such as, for example, 20 ksi, the estimate of maximum load due to the combined crookedness and residual stress may be grossly unsafe if residual stress is ignored.

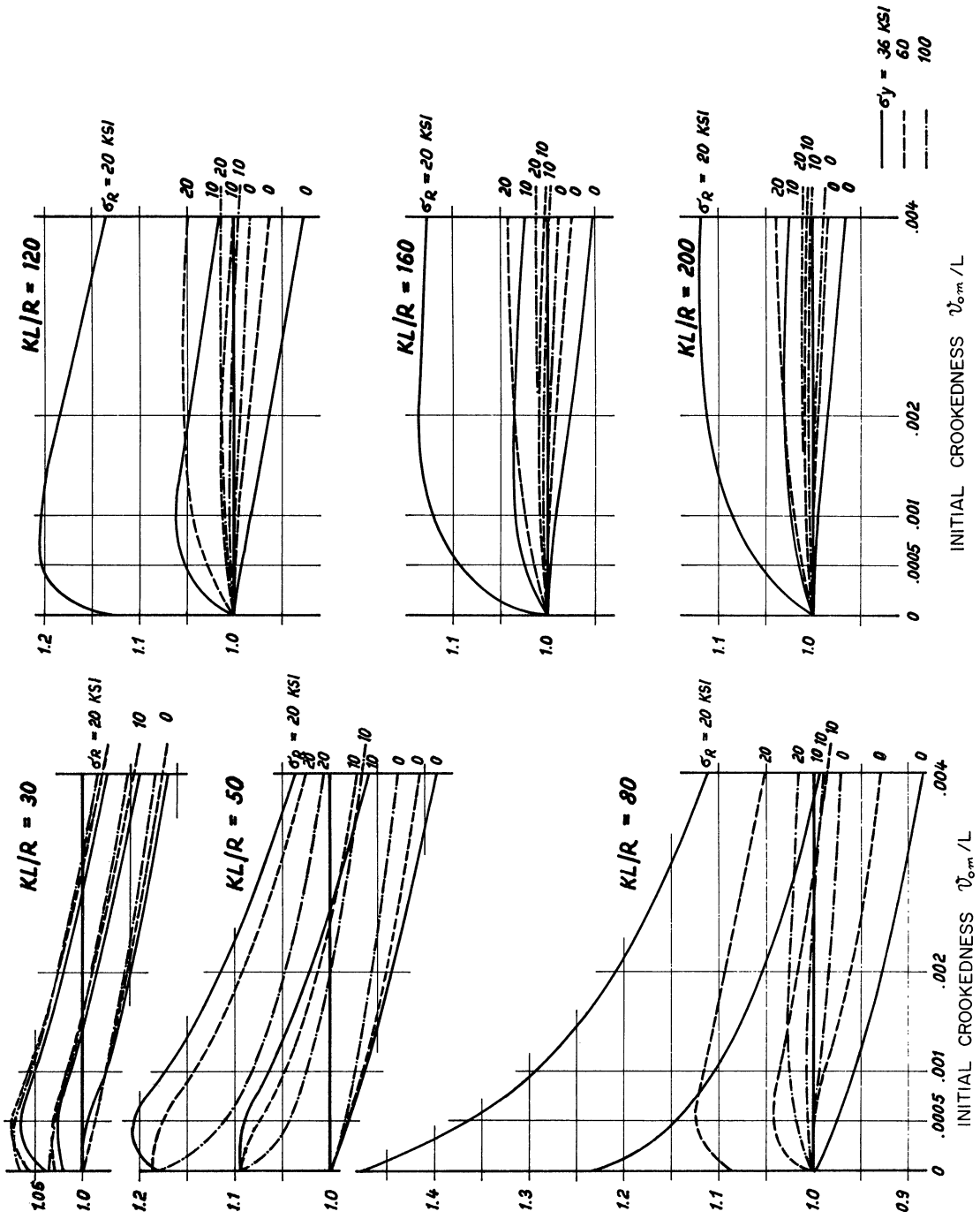

Figure 32. Relation between Maximum Column Strength and Load at Which a Column Free of the Residual Stress Reaches the yield Stress.

SUMMARY AND CONCLUSIONS

1. Maximum strengths of aluminum alloy and steel columns as influenced by various parameter variations are systematically determined by means of a mathematical model programmed for the 7090 computer.
2. The effects of initial crookedness on an aluminum alloy column and the effects of both initial crookedness and residual cooling stresses (alone or in combination) on the behavior of wide flange steel columns are systematically evaluated for yield points of 36, 60, and 100 ksi. Within the usual limits of variation of residual stress and crookedness magnitudes, the maximum column strength may be estimated by interpolation for any given residual stress magnitude, initial crookedness, slenderness ratio, or yield stress.
3. For idealized straight columns of either aluminum alloy or steel, the maximum inelastic post buckling strength is shown to be only a few per cent above the bifurcation (tangent modulus) load.
4. The maximum strength of short and intermediate length steel columns that are initially crooked may be appreciably above the column load that causes the maximum combined bending plus residual stress to reach the yield stress.
5. The current AISC design formula for centrally load steel columns provides a reasonably consistent load factor of safety with respect to the maximum strength of wide flange structural grade steel columns having a combined maximum residual stress of 10 ksi together with an initial crookedness of L/1000. For the same levels of combined residual stress and crookedness, in the case of the higher yield stress

steels of 60 ksi and 100 ksi, the same AISC formula is shown to be relatively more conservative than for the 36 ksi yield stress.

6. Reductions in strength caused by a combination of residual stresses and initial crookedness are not approximated accurately by superposing reductions caused by these factors acting separately.

7. An interaction formula for aluminum columns with initial crookedness was found to predict quite accurately the column strengths for the range of parameters covered in this project.

ACKNOWLEDGEMENTS

This investigation was initiated in 1962 when the first author was a graduate student at the University of Michigan. The work was largely unsponsored and the authors are grateful for the very large amount of computer time that has been made available through the Computing Center of the University of Michigan to make the final results possible. In bringing the work to a conclusion, the Bureau of Yards and Docks has provided support in the reduction of data and the Industry Program of the University of Michigan has assisted in the preparation of drawings. The continuation of the further development of the computer work at the University of Michigan subsequent to the departure of the first author was made possible through the assistance of Mr. Rafi Hariri. Assistance in reducing the data and in preparation of drawings has been rendered by Mr. Ernst Glauser. Both Mr. Hariri and Mr. Glauser are Research Assistants at the University of Michigan.